Inorganic Chemistry
Article

Inorg. Chem. **2010**, *49*, 5049–5062 **5049**
DOI: 10.1021/ic100138s

Synthesis, Characterization, Photophysical, and Anion-Binding Studies of Luminescent Heteroleptic Bis-Tridentate Ruthenium(II) Complexes Based on 2,6-Bis(Benzimidazole-2-yl)Pyridine and 4′-Substituted 2,2′:6′,2′′ Terpyridine Derivatives

Chanchal Bhaumik,[†] Shyamal Das,[†] Debasish Saha,[†] Supriya Dutta,[‡] and Sujoy Baitalik*,[†]

[†]*Department of Chemistry, Inorganic Chemistry Section, Jadavpur University, Kolkata 700032, India, and*
[‡]*Department of Inorganic Chemistry, Indian Association for the Cultivation of Science, Kolkata 700 032, India*

Received January 22, 2010

A series of heteroleptic tridentate ruthenium(II) complexes of composition $[(H_2pbbzim)Ru(tpy\text{-}X)](PF_6)_2$ (**1**−**7**), where $H_2pbbzim$ = 2,6-bis(benzimidazole-2-yl)pyridine and tpy-X = 4′-substituted terpyridine ligands with X = H, *p*-methyl phenyl ($PhCH_3$), *p*-bromomethylphenyl ($PhCH_2Br$), *p*-dibromomethylphenyl ($PhCHBr_2$), *p*-cyanomethylphenyl ($PhCH_2CN$), *p*-triphenylphosphonium methylphenyl bromide ($PhCH_2PPh_3Br$), and 4′-phenylformyl (PhCHO) groups, has been synthesized and characterized by using standard analytical and spectroscopic techniques. These compounds were designed to increase the excited-state lifetime of ruthenium(II) bisterpyridine-type complexes. The X-ray crystal structure of a representative compound **2**, which crystallized with monoclinic space group *P*2(1)/*c*, has been determined. The absorption spectra, redox behavior, and luminescence properties of the ruthenium(II) complexes have been thoroughly investigated. All of the complexes display moderately strong luminescence at room temperature with lifetimes in the range of 10−58 ns. Correlations have been obtained for the Hammett σ_p parameter with their MLCT emission energies, lifetimes, redox potentials, proton NMR chemical shifts, etc. The anion binding properties of all the complexes as well as the parent ligand $H_2pbbzim$ have been studied in acetonitrile using absorption, emission, and ^1H NMR spectral studies, and it has been observed that the metalloreceptors act as sensors for F^-, AcO^-, and to some extent $H_2PO_4^-$. At a relatively lower concentration of anions, a 1:1 H-bonded adduct is formed; however, in the presence of an excess of anions, stepwise deprotonation of the two benzimidazole N−H fragments occurs, an event which is signaled by the development of vivid colors visible with the naked eye. The receptor−anion binding constants have been evaluated. Cyclic voltammetric (CV) measurements carried out in acetonitrile−dimethylformamide (9:1) provided evidence in favor of anion (F^-, AcO^-) concentration dependent electrochemical responses, enabling **1** − **7** to act as suitable electrochemical sensors for F^- and AcO^- ions.

Introduction

Supramolecular chemistry of anion recognition and binding is a subject of considerable contemporary research interest.[1−10] Anions being ubiquitous, quite a few of them play important roles in biological, aquatic, environmental, and industrial processes.[1−10] Consequently, a lot of efforts have been directed toward the designing of receptors that can selectively recognize anions and act as sensors. A number of compounds containing urea, thiourea, amide, pyrrole, or imidazole subunits that are capable of providing hydrogen bond forming sites have been reported to exhibit strong affinity and selectivity toward certain anions.[1−12] When the metalloreceptor is designed to function

*To whom correspondence should be addressed: E-mail: sbaitalik@hotmail.com.

(1) Sessler, J. L.; Gale, P. A.; Cho, W. S. *Anion Receptor Chemistry*; Royal Society of Chemistry: Cambridge, U.K., 2006.
(2) (a) Beer, P. D.; Bayly, S. R. *Top. Curr. Chem.* **2005**, *255*, 125–162. (b) Caltagirone, C.; Gale, P. A. *Chem. Soc. Rev.* **2009**, *38*, 520–563. (c) Gale, P. A.; Garcia-Garrido, S. E.; Garric, J. *Chem. Soc. Rev.* **2008**, *37*, 151–190. (d) Gale, P. A. *Coord. Chem. Rev.* **2006**, *250*, 2917. (e) Sessler, J. L.; Davis, J. M. *Acc. Chem. Res.* **2001**, *34*, 989–997.
(3) Martínez-Máñez, R.; Sancenón, F. *Chem. Rev.* **2003**, *103*, 4419–4476.
(4) Steed, J. W. *Chem. Soc. Rev.* **2009**, *38*, 506–519.
(5) (a) dos Santos, C. M. G.; Harte, A. J.; Quinn, S. T.; Gunnalaugsson, T. *Coord. Chem. Rev.* **2008**, *252*, 2512–2527. (b) Gunnalaugsson, T.; Glynn, M.; Tocci (nee Hussey), G. M.; Kruger, P. E.; Pfeffer, F. M. *Coord. Chem. Rev.* **2006**, *250*, 3094–3117.
(6) (a) Peŕez, J.; Riera, L. *Chem. Commun.* **2008**, 533–543. (b) Peŕez, J.; Riera, L. *Chem. Soc. Rev.* **2008**, *37*, 2658–2667.
(7) Rice, C. R. *Coord. Chem. Rev.* **2006**, *250*, 3190–3199.
(8) (a) Kumar, A.; Sun, S.-S.; Lees, A. J. *Coord. Chem. Rev.* **2008**, *252*, 922–939. (b) Amendola, V.; Gómez, E. D.; Fabbrizzi, L.; Licchelli, M. *Acc. Chem. Res.* **2006**, *39*, 343–353. (c) Suksai, C.; Tuntulani., T. *Top. Curr. Chem.* **2005**, *255*, 163–198. (d) Amendola, V.; Fabbrizzi, L. *Chem. Commun.* **2008**, 513–531.
(9) Bianchi, A.; Bowman-James, K.; García-España. *Supramolecular Chemistry of Anions*; Wiley-VCH: New York, 1997.
(10) Prados, P.; Quesada, R. *Supramol. Chem.* **2008**, *20*, 201–216.
(11) (a) Gunnlaugsson, T.; Stomeo, F. *Org. Biomol. Chem.* **2007**, *5*, 1999–2009. (b) Leonard, J. P.; Nolan, C. B.; Stomeo, F.; Gunnlaugsson, T. *Top. Curr. Chem.* **2007**, *281*, 1–43.
(12) (a) Bondy, C. R.; Loeb, S. J. *Coord. Chem. Rev.* **2003**, *240*, 77–99. (b) Choi, K.; Hamilton, A. D. *Coord. Chem. Rev.* **2003**, *240*, 101–110. (c) Mizukami, S.; Nagano, T.; Urano, Y.; Odani, A.; Kikuchi, K. *J. Am. Chem. Soc.* **2002**, *124*, 3920–3925. (d) Lu, H.; Xu, W.; Zhang, D.; Zhu, D. *Chem. Commun.* **2005**, 4777–4779. (e) Cho, E. J.; Moon, J. W.; Ko, S. W.; Lee, J. Y.; Kim, S. K.; Yoon, J; Nam, K. C. *J. Am. Chem. Soc.* **2003**, *125*, 12376–12377. (f) Otón, F.; Tárraga, A.; Espinosa, A.; Velasco, M. D.; Molina, P. *J. Org. Chem.* **2006**, *71*, 4590–4598. (g) Otón, F.; Tárraga, A.; Velasco, M. D.; Espinosa, A.; Molina, P. *Chem. Commun.* **2004**, 1658–1659.

Published on Web 05/14/2010

as a sensor, metal fragments can be used as reporter units for modulating a signal, usually color, fluorescence, or electrochemical potentials, as a result of host−guest interaction.[3,4,6] In recent years, the development of multichannel sensors has emerged as a topic of intensive studies.[2−8] Inasmuch as ruthenium(II) polypyridine complexes are known to display unique photophysical and redox properties,[13−17] a number of ruthenium(II) polypyridine-based receptors have been designed as ion sensors,[18−23] although such sensors for anions are relatively few. In contrast to tris(bidentate) complexes, structurally more appealing $[Ru(tpy)_2]^{2+}$ type complexes give rod-like assemblies when substituted at the 4′ position of the tpy ligands.[24−27] However, usually such complexes are practically non-luminescent at room temperature and their excited state lifetime ($\tau = 0.25$ ns)[28] is also very short, and therefore these are the major deterrents for using them to act as photosensitizers. Consequently, much effort has been devoted to designing and synthesizing tridentate polypyridine ligands that can produce ruthenium(II) complexes with enhanced emission quantum yields and excited-state lifetimes. Most of the approaches aim to increase the energy gap between the radiative ^{3}MLCT and quenching ^{3}MC states. Stabilization of the ^{3}MLCT state can be achieved interalia by substitution of the tpy ligands by electron-withdrawing groups,[29] introducing a coplanar hetero-aromatic moiety,[30] incorporation of an organic chromophore, etc. Indeed, such approaches have produced complexes that have longer emission lifetimes compared to the parent compounds.[31−33] A second approach is to destabilize the ^{3}MC state by using cyclometalated ligands.[34−36] One can also modify the terpyridine directly, by replacing the pyridines with other heterocyclic rings to enlarge the bite angle of the tridentate ligand.[37] Although the spectroscopic and electrochemical properties of a few ruthenium(II) complexes containing

(13) Meyer, T. J. *Pure Appl. Chem.* **1986**, *58*, 1193–1206.
(14) (a) Juris, A.; Balzani, V.; Barigelletti, F.; Campagna, S.; Belser, P.; von Zelewsky, A. *Coord. Chem. Rev.* **1988**, *84*, 85–277. (b) Balzani, V.; Juris, A.; Venturi, M.; Campagna, S.; Serroni, S. *Chem. Rev.* **1996**, *96*, 759–834.
(15) Sauvage, J.-P.; Collin, J. P.; Chambron, J. C.; Guillerez, S.; Coudret, C.; Balzani, V.; Barigelletti, F.; De Cola, L.; Flamigni, L. *Chem. Rev.* **1994**, *94*, 993–1019.
(16) Baranoff, E.; Collin, J. P.; Flamigni, L.; Sauvage, J.-P. *Chem. Soc. Rev.* **2004**, *33*, 147–155.
(17) (a) Baitalik, S.; Wang, X.; Schmehl, R. H. *J. Am. Chem. Soc.* **2004**, *126*, 16304–16305. (b) Baitalik, S.; Flörke, U.; Nag, K. *Inorg. Chem.* **1999**, *38*, 3296–3308. (c) Baitalik, S.; Flörke, U.; Nag, K. *J. Chem. Soc., Dalton Trans.* **1999**, 719–717. (d) Baitalik, S.; Bag, P.; Flörke, U.; Nag, K. *Inorg. Chim. Acta* **2004**, *357*, 699–706.
(18) (a) Saha, D.; Das, S.; Bhaumik, C.; Dutta, S.; Baitalik, S. *Inorg. Chem.* **2010**, *49*, 2334–2348. (b) Das, S.; Saha, D.; Bhaumik, C.; Dutta, S.; Baitalik, S. *Dalton Trans.* **2010**, *39*, 4162–4169.
(19) (a) Anzebacher, P.; Tyson, D. S.; Jurslkova, K.; Castellano, F. N. *J. Am. Chem. Soc.* **2002**, *124*, 6232–6233. (b) Mizuno, T.; Wei, W.-H.; Eller, L. R.; Sessler, J. L. *J. Am. Chem. Soc.* **2002**, *124*, 1134–1135.
(20) (a) Beer, P. D.; Szemes, F.; Balzani, V.; Salà, C. M.; Drew, M. G. B.; Dent, S. W.; Maestri, M. *J. Am. Chem. Soc.* **1997**, *119*, 11864–11875. (b) Beer, P. D.; Graydon, A. R.; Sutton, L. R. *Polyhedron* **1996**, *15*, 2457–2461. (c) Beer, P. D.; Szemes, F. *J. Chem. Soc., Chem. Commun.* **1995**, 2245–2247. (d) Beer, P. D.; Dent, S. W.; Fletcher, N. C.; Wear, T. J. *Polyhedron* **1996**, *15*, 2983–2996. (e) Beer, P. D.; Timoshenko, V.; Maestri, M.; Passaniti, P.; Balzani, V. *Chem. Commun.* **1999**, 1755–1756. (f) Szemes, F.; Hesek, D.; Chen, Z.; Dent, S. W.; Drew, M. G. B.; Goulden, A. J.; Graydon, A. R.; Grieve, A.; Mortimer, R. J.; Wear, T. J.; Weightman, J. S.; Beer, P. D. *Inorg. Chem.* **1996**, *35*, 5868–5879.
(21) (a) Cui, Y.; Mo, H.-J.; Chen, J.-C.; Niu, Y.-L.; Zhong, Y.-R.; Zheng, K.-C.; Ye, B.-H. *Inorg. Chem.* **2007**, *46*, 6427–6436. (b) Cui, Y.; Niu, Y.-L.; Cao, M. L.; Wang, K.; Mo, H.-J.; Zhong, Y.-R.; Ye, B.-H. *Inorg. Chem.* **2008**, *47*, 5616–5624. (c) Lin, Z.-H.; Ou, S.-J.; Duan, C.-Y.; Zhang, B.-G.; Bai, Z.-P. *Chem. Commun.* **2006**, 624–626. (d) Lin, Z.-H.; Zhao, Y.-G.; Duan, C.-Y.; Zhang, B.-G.; Bai, Z.-P. *Dalton Trans.* **2006**, 3678–3684.
(22) (a) Ion, L.; Morales, D.; Perez, J.; Riera, L.; Riera, V.; Kowenicki, R. A.; McPartlin, M. *Chem. Commun.* **2006**, 91–93. (b) Zapata, F.; Caballero, A.; Espinosa, A.; Tárraga, A.; Molina, P. *J. Org. Chem.* **2008**, *73*, 4034–4044. (c) Derossi, S.; Adams, H.; Ward, M. D. *Dalton Trans.* **2007**, 33–36. (d) Lazarides, T.; Miller, T. A.; Jeffery, J. C.; Ronson, T. K.; Adams, H.; Ward, M. D. *Dalton Trans.* **2005**, 528–536. (e) Jose, D. A.; Kar, P.; Koley, D.; Ganguly, B.; Thiel, W.; Ghosh, H. N.; Das, A. *Inorg. Chem.* **2007**, *46*, 5576–5584. (f) Rau, S.; Buttner, T.; Temme, C.; Ruben, M.; Gorls, H.; Walther, D.; Duati, M.; Fanni, S.; Vos, J. G. *Inorg. Chem.* **2000**, *39*, 1621–1624. (g) Fortin, S.; Beauchamp, A. L. *Inorg. Chem.* **2001**, *40*, 105–112.
(23) (a) Watanabe, S.; Onogawa, O.; Komatsu, Y.; Yoshida, K. *J. Am. Chem. Soc.* **1998**, *120*, 229–230. (b) Aoki, S.; Zulkefeli, M.; Shiro, M.; Kohsako, M.; Takeda, K.; Kimura, E. *J. Am. Chem. Soc.* **2005**, *127*, 9129–9139. (c) Lin, T.-P.; Chen, C.-Y.; Wen, Y.-S.; Sun, S.-S. *Inorg. Chem.* **2007**, *46*, 9201–9212. (d) Wu, C.-Y.; Chen, M.-S.; Lin, C.-A.; Lin, S.-C.; Sun, S.-S. *Chem.—Eur. J.* **2006**, *12*, 2263–2269.
(24) Constable, E. C. *Chem. Soc. Rev.* **2004**, *33*, 246–253.
(25) Hofmeier, H.; Schubert, U. S. *Chem. Soc. Rev.* **2004**, *33*, 373–399.
(26) (a) Medlycott, E. A.; Hanan, G. S. *Coord. Chem. Rev.* **2006**, *250*, 1763–1782. (b) Medlycott, E. A.; Hanan, G. S. *Chem. Soc. Rev.* **2005**, *34*, 133–142.
(27) (a) Wang, X.-Y.; Del Guerzo, A.; Schmehl, R. H. *J. Photochem. Photobiol. C* **2004**, *5*, 55–77. (b) Baba, A. I.; Shaw, J. R.; Simon, J. A.; Thummel, R. P.; Schmehl, R. H. *Coord. Chem. Rev.* **1998**, *171*, 43–59.
(28) Winkler, J. R.; Netzel, T.; Creutz, C.; Sutin, N. *J. Am. Chem. Soc.* **1987**, *109*, 2381–2392.
(29) (a) Maestri, M.; Armaroli, N.; Balzani, V.; Constable, E. C.; Thompson, A. M. W. C. *Inorg. Chem.* **1995**, *34*, 2759–2767. (b) Constable, E. C.; Cargill Thompson, A. M. W.; Armaroli, N.; Balzani, V.; Maestri, M. *Polyhedron* **1992**, *11*, 2707–2709. (c) Wang, J.; Fang, Y. Q.; Hanan, G. S.; Loiseau, F.; Campagna, S. *Inorg. Chem.* **2005**, *44*, 5–7.
(30) (a) Fang, Y. Q.; Taylor, N. J.; Laverdiere, F.; Hanan, G. S.; Loiseau, F.; Nastasi, F.; Campagna, S.; Nierengarten, H.; Leize-Wagner, E.; Van Dorsselaer, A. *Inorg. Chem.* **2007**, *46*, 2854–2863. (b) Fang, Y. Q.; Taylor, N. J.; Hanan, G. S.; Loiseau, F.; Passalacqua, R.; Campagna, S.; Nierengarten, H.; Van Dorsselaer, A. *J. Am. Chem. Soc.* **2002**, *124*, 7912–7913.
(31) (a) Polson, M. I. J.; Loiseau, F.; Campagna, S.; Hanan, G. S. *Chem. Commun.* **2006**, 1301–1303. (b) Passalacqua, R.; Loiseau, F.; Campagna, S.; Fang, Y. Q.; Hanan, G. S. *Angew. Chem., Int. Ed.* **2003**, *42*, 1608–1611.
(32) (a) Encinas, S.; Flamigni, L.; Barigelletti, F.; Constable, E. C.; Housecroft, C. E.; Schofield, E. R.; Figgemeier, E.; Fenske, D.; Neuburger, M.; Vos, J. G.; Zehnder, M. *Chem.—Eur. J.* **2002**, *8*, 137–150. (b) Hammarström, L.; Barigelletti, F.; Flamigni, L.; Indelli, M. T.; Armaroli, N.; Calogero, G.; Guardigli, M.; Sour, A.; Collin, J.-P.; Sauvage, J.-P. *J. Phys. Chem. A* **1997**, *101*, 9061–9069.
(33) (a) Hissler, M.; El-ghayoury, A.; Harriman, A.; Ziessel, R. *Angew. Chem., Int. Ed.* **1998**, *37*, 1717–1720. (b) Benniston, A. C.; Grosshenny, V.; Harriman, A.; Ziessel, R. *Angew. Chem., Int. Ed.* **1994**, *33*, 1884–1885. (c) Benniston, A. C.; Harriman, A.; Li, P.; Sams, C. A. *J. Am. Chem. Soc.* **2005**, *127*, 2553–2564. (d) Wang, X-y.; Del Guerzo, A.; Tunuguntla, H.; Schmehl, R. H. *Res. Chem. Intermed.* **2007**, *33*, 63–77.
(34) (a) Duati, M.; Tasca, S.; Lynch, F. C.; Bohlen, H.; Vos, J. G.; Stagni, S.; Ward, M. D. *Inorg. Chem.* **2003**, *42*, 8377–8384. (b) Duati, M.; Fanni, S.; Vos, J. G. *Inorg. Chem. Commun.* **2000**, *3*, 68–70.
(35) (a) Indelli, M. T.; Bignozzi, C. A.; Scandola, F.; Collin, J.-P. *Inorg. Chem.* **1998**, *37*, 6084–6089. (b) Constable, E. C.; Dunne, S. J.; Rees, D. G. F.; Schmitt, C. X. *Chem. Commun.* **1996**, 1169–1170.
(36) (a) Beley, M.; Collin, J.-P.; Louis, R.; Metz, B.; Sauvage, J.-P. *J. Am. Chem. Soc.* **1991**, *113*, 8521–8522. (b) Beley, M.; Collin, J.-P.; Sauvage, J.-P. *Inorg. Chem.* **1993**, *32*, 4539–4543. (c) Wilkinson, A. J.; Puschmann, H.; Howard, J. A. K.; Foster, C. E.; Williams, J. A. G. *Inorg. Chem.* **2006**, *45*, 8685–8699. (d) Beley, M.; Chodorowski, S.; Collin, J.-P.; Sauvage, J.-P.; Flamigni, L.; Barigelletti, F. *Inorg. Chem.* **1994**, *33*, 2543–2547. (e) Wadman, S. H.; Lutz, M.; Tooke, D. M.; Spek, A. L.; Hartl, F.; Havenith, R.W. A.; van Klink, G. P. M.; van Koten, G. *Inorg. Chem.* **2009**, *48*, 1887–1900.
(37) (a) Abrahamsson, M.; Lundqvist, M. J.; Wolpher, H.; Johansson, O.; Eriksson, L.; Bergquist, J.; Rasmussen, T.; Becker, H.-C.; Hammarström, L.; Norrby, P.-O.; Åkermark, B.; Persson, P. *Inorg. Chem.* **2008**, *47*, 3540–3548. (b) Abrahamsson, M.; Jäger, M.; Österman, T.; Eriksson, L.; Persson, P.; Becker, H. C.; Johansson, O.; Hammarström, L. *J. Am. Chem. Soc.* **2006**, *128*, 12616–12617. (c) Abrahamsson, M.; Jäger, M.; Kumar, R. J.; Österman, T.; Persson, P.; Becker, H. C.; Johansson, O.; Hammarström, L. *J. Am. Chem. Soc.* **2008**, *130*, 15533–15542.

Chart 1

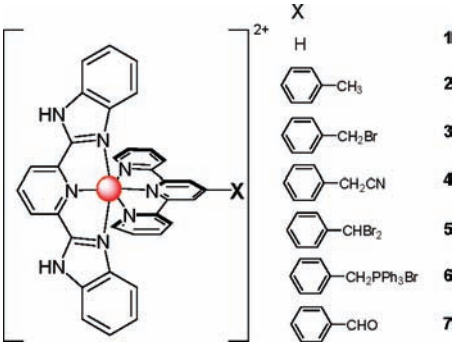

H_2pbbzim and terpyridine derivatives have been reported,[38−40] a systematic study dealing with the receptor behavior of these complexes for various anions is lacking. To this end, we report herein a new series of luminescent heteroleptic bis-tridentate ruthenium(II) complexes by using H_2pbbzim and different 4′-substituted terpyridine derivatives for multichannel recognition of ions such as F^-, AcO^-, and to some extent $H_2PO_4^-$. To allow fine-tuning of the electronic properties, several electron withdrawing substituents have been introduced in the 4′ position of each tpy ligand, resulting in seven complexes as shown in Chart 1. As will be seen, the most striking feature of these ruthenium(II) complexes is their fairly strong room temperature luminescence and appreciably long excited state lifetimes.

Experimental Section

Materials. Reagent grade chemicals obtained from commercial sources were used as received. Solvents were purified and dried according to standard methods. 2,2′:6′,2″-Terpyridine (tpy), 2,6-pyridinedicarboxylic acid, 1,2-phenylenediamine, and the tetrabutylammonium (TBA) salt of the anions were purchased from Sigma−Aldrich. 4′-(*p*-Methylphenyl)-2,2′:6′,2″-terpyridine (tpy-$PhCH_3$), 4′-(*p*-bromomethylphenyl)-2,2′:6′,2″-terpyridine (tpy-$PhCH_2Br$),[41,42] 4′-(*p*-dibromomethylphenyl)-2,2′:6′,2″−terpyridine(tpy -$PhCHBr_2$), 4′-(*p*- cyanomethylphenyl)-2,2′:6′,2″-terpyridine (tpy-$PhCH_2CN$), [4′-(*p* -triphenylphosphoniummethylphenyl)-2,2′:6′,2″-terpyridine]bromide (tpy −$PhCH_2PPh_3Br$), 4′-formyl-2,2′:6′,2″-terpyridine (tpy −PhCHO), [43] and 2,6-bis(benzimidazole-2-yl)-pyridine (H_2pbbzim)[44] were synthesized according to the literature procedures. [$Ru(H_2pbbzim)Cl_3$] was prepared by the reaction of $RuCl_3 \cdot 3H_2O$ with H_2pbbzim in refluxing ethanol.

Synthesis of the Ligands. 4′-(*p*-Tolyl)-2,2′:6′,2″-terpyridine (tpy-$PhCH_3$). The synthesis of tpy-$PhCH_3$ was undertaken by following a method previously described.[41,42] A mixture 2-acetylpyridine (12.5 g, 0.10 mol), *p*-tolualdehyde (6.2 g, 0.05 mol), acetamide (92.0 g, 1.6 mol), and ammonium acetate (59.0 g, 0.76 mol) was stirred at reflux for 2 h. The reaction mixture was cooled to 120 °C; then a solution of NaOH (10 g) in water (100 mL) was added, and refluxing was continued for a further 2 h. At room temperature, the black, rubber-like solid that formed was filtered off and washed with water and then with ethanol. The raw product was then recrystallized from ethanol. Further purification was performed through basic activated alumina column chromatography with a mixture of hexane and ethyl acetate (8:1) as the eluent. At this stage, ^{1}H NMR revealed the presence of two compounds. The needles thus obtained (6.0 g) were dissolved in an ethanol−dichloromethane mixture (1:1, 200 mL), and an ethanol solution of ferrous perchlorate (2.72 g in 50 mL) was added to give immediately a violet crystalline compound. The precipitate was collected and washed with toluene (3 × 100 mL). Characterization of the isolated precipitate (elemental analysis, ^{1}H NMR, cyclic voltammetry) confirms the formula [$Fe(tpy\text{-}PhCH_3)_2(ClO_4)_2$]. tpy-$PhCH_3$ was liberated from the complex by oxidation of the Fe(II) complex by H_2O_2 in an alkaline medium following the procedure described by Constable et al.[45] This afforded 4.0 g of tpy-$PhCH_3$, 24% yield. ^{1}H NMR ($CDCl_3$): δ (ppm) 2.42 (s, 3H), 7.31 (d, 2H, J = 8.0 Hz), 7.36 (tt, 2H, J = 5.2 Hz, J = 0.8 Hz), 7.82 (d, 2H, J = 8.0 Hz), 7.87 (tt, 2H J = 5.6 Hz, J = 1.6 Hz), 8.66 (d, 2H, J = 8.0 Hz), 8.71 (d, 2H J = 8.0 Hz), 8.73 (s, 2H). ^{13}C NMR ($CDCl_3$): δ (ppm) 21.21, 118.64, 118.70, 121.34, 121.59, 123.80, 127.08, 127.24, 129.52, 129.73, 135.71, 136.85, 139.04, 149.08, 149.13, 150.21, 155.90, 156.45.

4′-(*p*-Bromomethylphenyl)-2,2′:6′,2″-terpyridine (tpy-$PhCH_2Br$). A mixture of 4′-(*p*−tolyl)-2,2′:6′,2″-terpyridine (tpy-$PhCH_3$; 1.00 g, 3.09 mmol), N-bromosuccinamide (0.56 g, 3.09 mmol), and benzoyl peroxide (0.025 g, 0.10 mmol) in CCl_4 (20 mL) was heated at reflux for 8 h under N_2 protection and then cooled down to room temperature. The solid that formed was filtered and washed with dichloromethane (20 mL). The filtrate along with the washings was rotary evaporated, and the solid residue obtained was recrystallized from ethanol−acetone (3:1) mixture. The resulting solid was collected and washed with cold ethanol. Yield: 0.48 g (39%). ^{1}H NMR ($CDCl_3$): δ (ppm) 4.49 (s, 2H, CH_2Br), 7.27−7.30 (m, 2H), 7.46 (d, 2H, J = 8.0 Hz), 7.79−7.83 (m, 4H), 8.60 (d, 2H, J = 8.0 Hz), 8.70−8.72 (m, 4H). ^{13}C NMR ($CDCl_3$): δ (ppm) 33.24, 119.08, 121.69, 124.19, 128.00, 129.88, 137.34, 138.67, 138.86, 149.22, 149.73, 156.02, 156.12

4′-(*p*-Dibromomethylphenyl)-2,2′:6′,2″-terpyridine (tpy-$PhCHBr_2$). A mixture of 4′-(*p*-tolyl)-2,2′:6′,2″-terpyridine (tpy-$PhCH_3$; 1.00 g, 3.09 mmol), N-bromosuccinamide (1.23 g, 6.18 mmol), and benzoyl peroxide (0.049 g, 0.20 mmol) in CCl_4 (20 mL) was heated at reflux for 24 h under N_2 protection. After removal of CCl_4, the residue obtained was recrystallized by dissolving it in 50 mL of an ethanol−acetone (3:1) mixture and then keeping it in a refrigerator overnight. The solid was collected and washed with cold ethanol. Yield: 1.2 g (80%). ^{1}H NMR ($CDCl_3$): δ (ppm) 6.73 (s, 1H, $CHBr_2$), 7.37−7.40 (m, 2H), 7.73(d, 2H, J = 8.8 Hz), 7.72−7.94 (m, 4H), 8.69 (d, 2H, J = 8.0 Hz), 8.73−8.77 (m, 4H). ^{13}C NMR ($CDCl_3$): δ(ppm) 40.58, 119.37, 121.78, 124.31, 127.41, 127.91, 137.49, 140.13, 142.79, 149.18, 149.33, 155.96, 156.04.

(38) (a) Padilla-Tosta, M. E.; Lloris, J. M.; Martínez-Máñez, R.; Pardo, T.; Soto, J.; Benito, A.; Marcos, M. D. *Inorg. Chem. Commun.* **2000**, *3*, 45–48. (b) Padilla-Tosta, M. E.; Lloris, J. M.; Martínez-Máñez, R.; Pardo, T.; Sancenón, F.; Soto, J.; Marcos, M. D. *Eur. J. Inorg. Chem.* **2001**, 1221–1226. (c) Licini, M.; Williams, J. A. G. *Chem. Commun.* **1999**, 1943–1944. (d) Hamilton, A. D.; Linton, B. *Chem. Rev.* **1997**, *97*, 1669–1680. (e) Goodman, M. S.; Jubian, V.; Linton, B.; Hamilton, A. D. *J. Am. Chem. Soc.* **1995**, *117*, 11610–11611.

(39) (a) Yam, V. W. W. *Acc. Chem. Res.* **2002**, *35*, 555–563. (b) Wong, K. M. C.; Tang, W. S.; Lu, X. X.; Zhu, N.; Yam, V. W. W. *Inorg. Chem.* **2005**, *44*, 1492–1498. (c) Yam, V. W. W.; Tang, R. P. L.; Wong, K. M. C.; Lu, X. X.; Cheung, K. K.; Zhu, N. *Chem.—Eur. J.* **2002**, *8*, 4066–4076. (d) Yam, V. W. W.; Wong, K. M. C.; Zhu, N. *Angew. Chem., Int. Ed.* **2003**, *42*, 1400–1403.

(40) (a) Xiaoming, X.; Haga, M.; Inoue, T. M.; Ru, Y.; Addison, A. W.; Kano, K. *J. Chem. Soc., Dalton Trans.* **1993**, 2477–2484. (b) Haga, M.; Takasugi, T.; Tomie, A.; Ishizuya, M.; Yamada, T.; Hossain, M. D.; Inoue, M. *Dalton Trans.* **2003**, 2069–2079. (c) Singh, A.; Chetia, B.; Mobin, S. M.; Das, G.; Iyer, P. K.; Mondal, B. *Polyhedron* **2007**, *27*, 1983–1988. (d) Mishra, D.; Barbieri, A.; Sabatini, C.; Drew, M. G. B.; Figgie, H. M.; Sheldrick, W. S.; Chattopadhyay, S. K. *Inorg. Chim. Acta* **2007**, *360*, 2231–2244. (e) Yang, H.; Chen, W.-T.; Qiu, D.-F.; Bao, X.-Y.; Xing, W.-R.; Liu, S.-S. *Huaxue Xuebao* **2007**, *65*, 2959–2964.

(41) Case, F. H.; Kaspen, T. J. *J. Am. Chem. Soc.* **1956**, *78*, 5842–5844.

(42) Spahni, W.; Calzaferri, G. *Helv. Chim. Acta* **1984**, *67*, 450–454.

(43) Pott, K. T.; Usifer, D. A.; Abruna, H. D. *J. Am. Chem. Soc.* **1987**, *109*, 3961–3967.

(44) (a) Addison, A. W.; Burke, P. *J. Heterocycl. Chem.* **1981**, *18*, 803–805. (b) Addison, A. W.; Rao, T. N.; Wahlgren, C. G. *J. Heterocycl. Chem.* **1983**, *20*, 1481–1484.

(45) Constable, E. C.; Ward, M. D.; Corr, S. *Inorg. Chim. Acta* **1988**, *141*, 201–203.

[4′-(*p*-Triphenylphosphoniummethylphenyl)-2,2′:6′,2″-terpyridine] Bromide (tpy-PhCH$_2$PPh$_3$Br). A mixture of 4′-(*p*-bromomethylphenyl)-2,2′:6′,2″-terpyridine (tpy-PhCH$_2$Br; 0.372 g, 0.93 mmol) and triphenylphosphine (0.606 g, 2.31 mmol) in toluene (25 mL) was heated at reflux for 10 h and then cooled down to room temperature. The white precipitate that was obtained was filtered off and washed thoroughly with toluene and then dried under a vacuum. This afforded the phosphonium salt (tpy-PhCH$_2$PPh$_3$Br) as a white solid (0.53 g, 86% yield). ^{1}HNMR (CDCl$_3$): δ (ppm) 5.55 (d, 2H, J = 14.4 Hz, −CH$_2$PPh$_3$), 7.20 (d, 2H, J = 8.0 Hz,), 7.26 (t, 2H, J = 6.4 Hz), 7.51 (d, 2H, J = 8.0 Hz), 7.50−7.80 (m, 17H), 8.45 (s, 2H), 8.51(d, 2H, J=8.0 Hz), 8.59 (d, 2H, J=4.4 Hz). ^{13}C NMR (CDCl$_3$): δ(ppm) 117.60, 118.46, 118.92, 121.66, 124.15, 127.79, 128.43, 130.63, 132.39, 134.73, 134.63, 135.22, 137.33, 149.17, 155.99, 158.34, 159.29.

4′-(*p*-Cyanomethylphenyl)-2,2′:6′,2″-terpyridine (tpy-PhCH$_2$CN). A mixture of 4′-(*p*-bromomethylphenyl)-2,2′:6′,2″ terpyridine (tpy-PhCH$_2$Br; 0.402 g, 1.0 mmol), NaCN (0.049 g, 1.0 mmol), and 20 mL of DMF was stirred magnetically for 10 h at room temperature. The resulting mixture was added to 100 mL of water and then extracted with CH$_2$Cl$_2$ (2 × 30 mL). After removing solvent, the crude product was purified by recrystallization from a dichloromethane−hexane (1:10) mixture. This gave the product tpy-PhCH$_2$CN (0.29 g, 83% yield). ^{1}H NMR (CDCl$_3$): δ (ppm) 3.83 (s, 2H, −CH$_2$CN), 7.32−7.35 (m, 2H), 7.3−7.36 (m, 2H), 7.47 (d, 2H, J=8.0 Hz), 7.87 (td, 2H, J=8.0 Hz, J = 2.0 Hz), 7.90 (d, 2H, J = 7.6 Hz), 8.66 (d, 2H, J = 8.0 Hz), 8.70−8.72 (m, 2H). ^{13}C NMR (CDCl$_3$): δ (ppm) 23.68, 117.88 (CN−), 118.98, 121.63, 124.19, 128.30, 128.73, 130.87, 137.21, 138.62, 149.35, 149.52, 156.25.

4′-(*p*-Formylphenyl)-2,2′:6′,2″-terpyridine (tpy-PhCHO). A suspension of 4′-(*p*-dibromomethylphenyl)-2,2′:6′,2″-terpyridine (tpy-PhCHBr$_2$) (0.45 g, 0.93 mmol) and CaCO$_3$ (1.00 g, 10 mmol) in a mixture of 1,4-dioxane−water (4:1, 50 mL) was heated at reflux for 30 h. The resulting mixture was then filtered. The filtrate was extracted with CH$_2$Cl$_2$ (2 × 50 mL). The extracts were combined and washed successively with a 0.1 M aqueous EDTA solution (50 mL), 0.1 M aqueous HCl (50 mL), and then with water (2 × 50 mL). Solvent was removed on a rotary evaporator after drying over anhydrous sodium sulfate. This furnished product tpy-PhCHO (0.26 g, 77% yield). ^{1}H NMR (CDCl$_3$): δ (ppm) 7.32−7.35 (m, 2H), 7.86 (t, 2H, J = 7.6 Hz,), 7.96−8.03 (q, 4H, J = 8.8 Hz,), 8.64 (d, 2H, J=8.0 Hz,), 8.68 (d, 2H, J=7.6 Hz,), 8.73 (s, 2H), 10.05 (s, 1H). ^{13}C NMR (CDCl$_3$): δ (ppm) 119.15, 121.58, 124.27, 128.21, 130.49, 136.61, 137.17, 144.59, 148.97, 149.37, 156.02, 156.37, 192.07.

Synthesis of the Metal Complexes. The complexes were prepared under oxygen and moisture-free dinitrogen using standard Schlenk techniques.

General Procedure for Preparation of Heteroleptic Ruthenium(II) Complexes [(H$_2$pbbzim)Ru(tpy-X)](PF$_6$)$_2$ (1−7). [(H$_2$pbbzim)-RuCl$_3$] (100 mg, 0.19 mmol) was suspended into ethylene glycol (30 mL) and heated at 100 °C with continuous stirring. To the suspension was added 0.20 mmol of different 4′-substituted 2,2′:6′,2″-terpyridines (tpy-X), and the reaction mixture was heated at 200 °C under nitrogen protection for 24 h. The resulting solution was cooled, and the hexafluorophosphate salt of the complexes was precipitated by pouring the solution into an aqueous solution of NH$_4$PF$_6$ (0.50 g in 10 mL of water). The precipitate obtained was filtered and washed with water and then ether and dried under a vacuum. The compound was then purified by silica gel column chromatography using a mixture of CH$_3$CN and 10% aqueous KNO$_3$ (10:1) as the eluent, followed by a subsequent anion exchange reaction with NH$_4$PF$_6$ to give the desired compound. The compound was finally recrystallized from an acetonitrile−methanol (1:1) mixture in the presence of a few drops of aqueous 10^{-4} M hexfluorophosphoric acid.

[(H$_2$pbbzim)Ru(tpy)](PF$_6$)$_2$ (1). Yield: 61%. Anal. calcd for $C_{34}H_{24}N_8P_2F_{12}Ru$: C, 43.65; H, 2.58; N, 11.97. Found: C, 43.51; H, 2.67; N, 11.85. ^{1}H NMR data {300 MHz, DMSO-d$_6$, SiMe$_4$, δ (ppm)}: 13.81 (s, 2H, NH (imidazole)), 9.15 (d, 2H, J = 8.1 Hz, H3), 8.73 (d, 4H, J = 8.2 Hz, 2H3′ + 2H11), 8.66 (t, 1H, J = 8.1 Hz, H10), 8.60 (t, 1H, J = 7.5 Hz, H4′), 7.89 (t, 2H, J = 7.8 Hz, H4), 7.63 (d, 2H, J = 8.2 Hz, H6), 7.46 (d, 2H, J = 5.4 Hz, H12), 7.22 (m, 4H, 2H5 + 2H13), 6.97 (t, 2H, J = 7.7 Hz, H14), 5.89 (d, 2H, J = 8.2 Hz, H15). ESI-MS (positive, CH$_3$CN): m/z 323.15 (100%) [(H$_2$pbbzim)Ru(tpy)]$^{2+}$; 645.29 (42%) [(Hpbbzim)Ru-(tpy)]$^+$. UV−vis [CH$_3$CN; λ_{max}, nm (ε, M^{-1} cm^{-1})]: 478 (15 700), 405 (9200), 348 (47 350), 313 (68 700), 271 (41 800).

[(H$_2$pbbzim)Ru(tpy-PhCH$_3$)](PF$_6$)$_2$ (2). Yield: 65%. Anal. calcd for $C_{41}H_{30}N_8P_2F_{12}Ru$: C, 48.01; H, 2.94; N, 10.92. Found: C, 47.92; H, 3.01; N, 10.85. ^{1}H NMR data {300 MHz, DMSO-d$_6$, SiMe$_4$, δ (ppm)}: 14.50 (s, 2H, NH (imidazole)), 9.54 (s, 2H, H3′), 9.0 (d, 2H, J = 8.1 Hz, H3), 8.78 (d, 2H, J = 7.9 Hz, H11), 8.6 (t, 1H, J = 7.7 Hz, H10), 8.48 (d, 2H, J=7.8 Hz, H8), 7.92 (t, 2H, J = 7.9 Hz, H4), 7.67- 7.59 (m, 4H, 2H6 + 2H7), 7.47 (d, 2H, J = 5.5 Hz, H12), 7.29−7.14 (m, 4H, 2H5 + 2H13), 6.99 (t, 2H, J=7.7 Hz, H14), 6.04 (d, 2H, J = 8.3 Hz, H15), 2.53 (s, 3H, H9). ESI-MS (positive, CH$_3$CN): m/z 367.95 (100%) [(H$_2$pbbzim)-Ru(tpy-PhCH$_3$)]$^{2+}$; 734.87 (40%) [(Hpbbzim)Ru(tpy-PhCH$_3$)]$^+$. UV−vis [CH$_3$CN; λ_{max}, nm (ε, M^{-1} cm^{-1})]: 487 (18 000), 405 (5100), 348 (34 500), 313 (56 300), 285 (48 300).

[(H$_2$pbbzim)Ru(tpy-PhCH$_2$Br)](PF$_6$)$_2$ (3). Yield: 41%. Anal. calcd for $C_{41}H_{29}N_8BrP_2F_{12}Ru$: C, 44.58; H, 2.64; N, 10.14. Found: C, 44.49; H, 2.70; N, 10.02. ^{1}H NMR data {300 MHz, DMSO-d$_6$, SiMe$_4$, δ (ppm)}: 14.75 (s, 2H, NH (imidazole)), 9.55 (s, 2H, H3′), 8.98 (d, 2H, J=8.0 Hz, H3), 8.73 (d, 2H, J=7.8 Hz, H8), 8.61−8.53 (m, 3H, 1H10 + 2H11), 7.92 (t, 2H, J=7.8 Hz, H4), 7.74 (d, 2H, J=8.0 Hz, H7), 7.62(d, 2H, J = 8.1 Hz, H6), 7.46 (d, 2H, J=5.3 Hz, H12), 7.22 (m, 4H, nr, 2H5 + 2H13), 6.96 (t, 2H, J=7.7 Hz, H14), 6.02 (d, 2H, J = 8.2 Hz, H15), 4.31 (s, 2H, H9). ESI−MS (positive, CH$_3$CN): m/z 407.31 (100%) [(H$_2$pbbzim)Ru(tpy-PhCH$_2$Br)]$^{2+}$; 813.71 (25%) [(Hpbbzim)-Ru(tpy-PhCH$_2$Br)]$^+$. UV−vis [CH$_3$CN; λ_{max}, nm (ε, M^{-1} cm^{-1})]: 488 (13 100), 405 (5300), 348 (28 400), 313 (40 500), 285 (28 500).

[(H$_2$pbbzim)Ru(tpy-PhCH$_2$CN)](PF$_6$)$_2$ (4). Yield: 40%. Anal. calcd for $C_{42}H_{29}N_9P_2F_{12}Ru$: C, 48.00; H, 2.78; N, 12.00. Found: C, 47.71; H, 2.89; N, 11.48. ^{1}H NMR data {300 MHz, DMSO-d$_6$, SiMe$_4$, δ (ppm)}: 14.70 (s, 2H, NH (imidazole)), 9.55 (s, 2H, H3′), 8.98 (d, 2H, nr, H3), 8.69 (d, 2H, J = 7.9 Hz, H8), 8.60−8.52 (m, 3H, 1H10 + 2H11), 7.91 (t, 2H, J = 7.1 Hz, H4), 7.77 (d, 2H, J = 8.2 Hz, H7), 7.60 (d, 2H, J = 8.1 Hz, H6), 7.45 (d, 2H, nr, H12), 7.23−7.13 (m, 4H, 2H5 + 2H13), 6.89 (t, 2H, J=7.4 Hz, H14), 5.97 (d, 2H, J=8.2 Hz, H15), 4. 72 (s, 2H, H9). ESI-MS (positive, CH$_3$CN): m/z 380.54 (100%) [(H$_2$pbb-zim)Ru(tpy-PhCH$_2$CN)]$^{2+}$; 760.13 (10%) [(Hpbbzim)Ru (tpy-PhCH$_2$CN)]$^+$. UV−vis [CH$_3$CN; λ_{max}, nm (ε, M^{-1} cm^{-1})]: 486 (19 900), 404 (6200), 348 (39 300), 314 (55 400), 285 (55 500).

[(H$_2$pbbzim)Ru(tpy-PhCHBr$_2$)](PF$_6$)$_2$ (5). Yield: 45%. Anal. calcd for $C_{41}H_{28}N_8Br_2P_2F_{12}Ru$: C, 41.60; H, 2.38; N, 9.46. Found: C, 41.59; H, 2.47; N, 9.41. ^{1}H NMR data {300 MHz, DMSO-d$_6$, SiMe$_4$, δ (ppm)}: 14.90 (s, 2H, NH (imidazole)), 9.53 (s, 2H, H3′), 8.97 (d, 2H, J = 8.0 Hz, H3), 8.60 (m, 4H, 2H8 + 2H11), 8.47 (t, 1H, J=7.9 Hz, H10), 7.89 (t, 2H, J=7.8 Hz, H4), 7.83 (d, 2H, J=7.2 Hz, H7), 7.53 (d, 2H, J = 8.0 Hz, H6), 7.44 (d, 2H, J=5.3 Hz, H12), 7.21 (t, 2H, J = 6.4 Hz, H5), 7.05 (t, 2H, J=6.5 Hz, H13), 6.79 (t, 2H, J = 7.7 Hz, H14), 5.93 (s, 1H, H9), 5.91 (d, 2H, J=8.1 Hz, H15). ESI-MS (positive, CH$_3$CN): m/z 446.75 (100%) [(H$_2$pbbzim)Ru(tpy-PhCHBr$_2$)]$^{2+}$; 892.57 (40%) [(Hpbbzim)Ru(tpy-PhCHBr$_2$)]$^+$. UV−vis [CH$_3$CN; λ_{max}, nm (ε, M^{-1} cm^{-1})]: 490 (23 500), 406 (7800), 348 (49 500), 314 (63 000), 286 (63 700).

[(H$_2$pbbzim)Ru(tpy-PhCH$_2$PPh$_3$Br)](PF$_6$)$_2$ (6). Yield: 48%. Anal. calcd for $C_{59}H_{44}N_8BrP_3F_{12}Ru$: C, 51.84; H, 3.24; N, 8.20. Found: C, 51.74; H, 3.28; N, 8.12. ^{1}H NMR data {300 MHz, DMSO-d$_6$, SiMe$_4$, δ (ppm)}: 14.80 (s, 2H, NH (imidazole)), 9.51 (s, 2H, H3′), 8.93 (d, 2H, J = 8.1 Hz, H3), 8.70 (m, 2H, H8), 8.56

(t, 1H, nr, H10), 8.50 (d, 2H, J = 8.1 Hz, H11), 7.99−7.77 (m, 17H, 2H4 + 15H(PPh_3)), 7.59 (d, 2H, J = 8.3 Hz, H7), 7.45 (d, 2H, J = 5.3 Hz, H12), 7.36 (d, 2H, J = 6.4 Hz, H6), 7.22 (t, 2H, J = 6.5 Hz, H5), 7.16 (t, 2H, J = 7.3 Hz, H13), 6.88 (t, 2H, J = 7.6 Hz, H14), 5.94 (d, 2H, J = 8.2 Hz, H15), 5.41 (s, 1H, H9), 5.36 (s, 1H, H9). ESI−MS (positive, CH_3CN): m/z 497.47 (100%) $[(H_2pbbzim)Ru(tpy\text{-}PhCHPPh_3)]^{2+}$. UV−vis [$CH_3CN$; λ_{max}, nm (ε, M^{-1} cm^{-1})]: 488 (22 600), 406 (7000), 348 (44 700), 313 (62 600), 286 (62 900).

[(H_2pbbzim)Ru(tpy-PhCHO)](PF_6)$_2$ (7). Yield: 51%. Anal. calcd for $C_{41}H_{28}N_8OP_2F_{12}Ru$: C, 47.36; H, 2.71; N, 10.77. Found: C, 47.02; H, 2.80; N, 10.45. ^{1}H NMR data {300 MHz, DMSO-d_6, $SiMe_4$, δ (ppm)}: 15.02 (s, 2H, NH (imidazole)), 10.26 (s, 1H, H9), 9.66 (s, 2H, H3′), 9.03 (d, 2H, J = 8.0 Hz, H3), 8.81 (d, 2H, J = 8.0 Hz, H8), 8.78 (d, J = 8.0 Hz, 2H, H11), 8.64 (t, 1H, J = 8.0 Hz, H10), 8.33 (d, 2H, J = 8.5 Hz, H7), 7.97 (t, 2H, J = 5.9 Hz, H4), 7.66 (d, 2H, J = 8.0 Hz, H6), 7.50 (d, 2H, J = 5.0 Hz, H12), 7.26 (t, 2H, J = 8.5 Hz, H13), 7.25 (t, 2H, J = 7.0 Hz, H5), 7.00 (t, 2H, J = 8.0 Hz, H14), 6.05 (d, 2H, J = 8.0 Hz, H15). ESI-MS (positive, CH_3CN): m/z 374.65 (100%) $[(H_2pbbzim)Ru(tpy\text{-}PhCHO)]^{2+}$; 748.32(22%) $[(Hpbbzim)Ru(tpy\text{-}PhCHO)]^{+}$. UV−vis [$CH_3CN$; λ_{max}, nm (ε, M^{-1} cm^{-1})]: 489 (18 100), 405 (6000), 347 (38 000), 315 (50 000), 287 (52 000).

Physical Measurements. Elemental (C, H, and N) analyses were performed on a Perkin−Elmer 2400II analyzer. Electrospray ionization mass spectra (ESI−MS) were obtained on a Micromass Qtof YA 263 mass spectrometer. ^{1}H and {^{1}H−^{1}H} COSY spectra were obtained on a Bruker Avance DPX 300 spectrometer using DMSO-d_6 solutions. For a typical titration experiment, 3 μL aliquots of a tetrabutylammonium (TBA) salt of the anion (0.2 M in DMSO-d_6) were added to a DMSO-d_6 solution of the complexes (2.5×10^{-3} M).

Electronic absorption spectra were obtained with a Shimadzu UV 1800 spectrophotometer at room temperature. For a typical titration experiment, 2 μL aliquots of TBA salts of F^-, Cl^-, Br^-, I^-, NO_3^-, and AcO^- and $H_2PO_4^-$ (4.0×10^{-3} M in acetonitrile) were added to a 2.5 mL solution of the complexes (2.0×10^{-5} M in acetonitrile). The binding constants were evaluated from the absorbance data using eq 1.[46]

$$A_{obs} = (A_0 + A_\infty K[G]_T)/(1 + K[G]_T) \quad (1)$$

where A_{obs} is the observed absorbance, A_0 is the absorbance of the free receptor, A_∞ is the maximum absorbance induced by the presence of a given anionic guest, $[G]_T$ is the total concentration of the guest, and K is the binding constant of the host−guest entity. Binding constants were performed in duplicate, and the average value is reported.

Emission spectra were recorded on Perkin−Elmer LS55 fluorescence spectrophotometer. The room temperature spectra were obtained in acetonitrile solutions, while the spectra at 77 K were recorded in 4:1 ethanol−methanol glass. Photoluminescence titrations were carried out with the same sets of solutions as were made with spectrophotometry. Quantum yields were determined by a relative method using $[Ru(bpy)_3]^{2+}$ in the same solvent as the standard.

Time-correlated single-photon-counting (TCSPC) measurements were carried out in acetonitrile for the luminescence decay of complexes **1**−**7**. For TCSPC measurement, the photoexcitation was made at 440 nm using a picosecond diode laser (IBH Nanoled−07) in an IBH Fluorocube apparatus. The fluorescence decay data were collected on a Hamamatsu MCP photomultiplier (R3809) and were analyzed by using IBH DAS6 software.

The electrochemical measurements were carried out with a BAS 100B electrochemistry system. A three-electrode assembly comprising a Pt (for oxidation) or glassy carbon (for reduction) working electrode, Pt auxiliary electrode, and an aqueous Ag/AgCl reference electrode were used. The cyclic voltammetric (CV) and square wave voltammetric (SWV) measurements were carried out at 25 °C in an acetonitrile solution of the complex (*ca.* 1 mM), and the concentration of the supporting electrolyte (TEAP) was maintained at 0.1 M. All of the potentials reported in this study were referenced against the Ag/AgCl electrode, which, under the given experimental conditions, gave a value of 0.36 V for the ferrocene/ferrocenium couple. For electrochemical titrations, 25 μL aliquots of TBA salts of the anions (2.0×10^{-2} M in acetonitrile) were added to a 5 mL (1.0×10^{-3} M) solution of sensors **1**−**7** in a acetonitrile−dimethylformamide (9:1) mixture.

Experimental uncertainties were as follows: absorption maxima, ± 2 nm; molar absorption coefficients, 10%; emission maxima, ± 5 nm; excited-state lifetimes, 10%; luminescence quantum yields, 20%; redox potentials, ± 10 mV.

X-Ray Crystal Structure Determination. Crystals suitable for structure determination were obtained by diffusing toluene to a solution of **2** in acetonitrile−dichloromethane (1:4). X-ray diffraction data for the crystal of **2** mounted on a glass fiber and coated with perfluoropolyether oil was collected at 296 K on a Bruker AXS SMART APEX II diffractometer equipped with a CCD detector using graphite-monochromated Mo Kα radiation (λ = 0.71073 Å). Crystallographic data and details of structure determination are summarized in Table 1. The data were processed with SAINT,[47] and absorption corrections were made with SADABS.[47] The structure was solved by direct and Fourier methods and refined by full-matrix least-squares on the basis of F^2 using the WINGX software, which utilizes SHELX-97.[48] For the structure solution and refinement, the SHELXTL software package[49] was used. The nonhydrogen atoms were refined anisotropically, while the hydrogen atoms were placed with fixed thermal parameters at idealized positions. In the structure of **2**, both the anionic perchlorates are severely disordered, and the structure was finally solved by removing the perchlorates by running the program SQUEEZE. The electron density map also showed the presence of some unassignable

Table 1. Crystallographic Data for $[(H_2pbbzim)Ru(tpy\text{-}PhCH_3)]^{2+}$ [**2**]$^{2+}$

	2
formula	$C_{41}H_{30}N_8Ru$
fw	735.80
T (K)	296(2)
cryst syst	monoclinic
space group	$P2(1)/c$
a (Å)	12.770(4)
b (Å)	16.303(5)
c (Å)	18.976(5)
α (deg)	90.00
β (deg)	104.121(4)
γ (deg)	90.00
V (Å^3)	3831.4(19)
D_c (g cm^{-3})	1.276
Z	4
μ (mm^{-1})	0.448
F(000)	1504
θ range (deg)	1.6 - 25.0
data/restraints/params	6738/0/451
GOF on F^2	1.065
R1 [$I > 2\sigma(I)$][a]	0.0689
wR2[b] (all data)	0.2358
$\Delta\rho_{max}/\Delta\rho_{min}$ (e Å)	1.35/-0.51

[a] $R1(F) = [\sum ||F_0| - |F_C||/\sum |F_0|]$. [b] $wR2\,(F^2) = [\sum w(F_0^2 - F_C^2)^2/\sum w(F_0^2)^2]^{1/2}$.

(46) Schneider, H.-J.; Yatsimirsky, A. *Principles and Methods in Supramolecular Chemistry*; John Wiley & Sons: England, 2000; p 142.

(47) *SAINT*, version 6.02; *SADABS*, version 2.03; Bruker AXS Inc.: Madison, WI, 2002.

(48) Sheldrick, G. M. *SHELXL-97*; University of Göttingen: Göttingen, Germany, 1997.

(49) *SHELXTL*, version 6.10; Bruker AXS Inc.: Madison, WI, 2002.

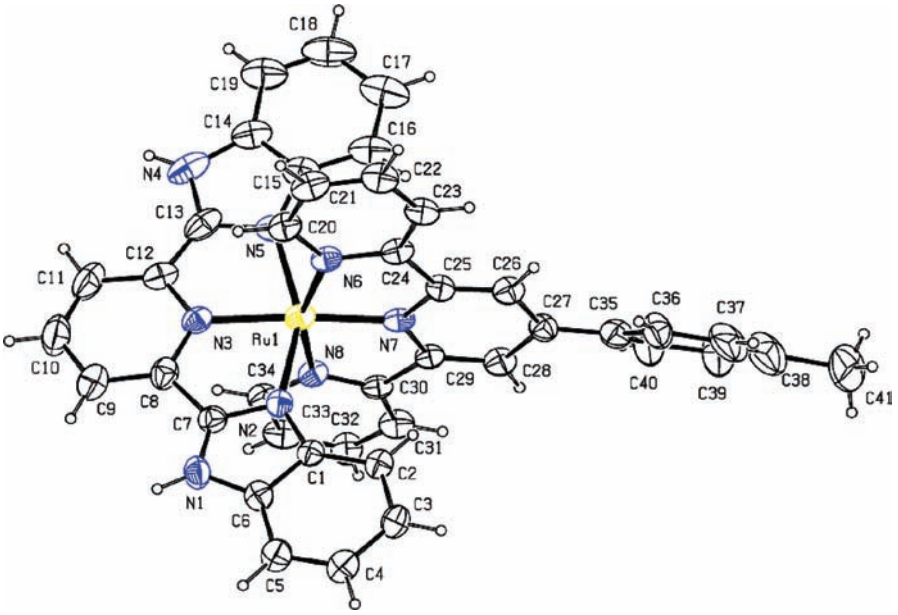

Figure 1. ORTEP representation of $[(H_2pbbzim)Ru(tpy\text{-}PhCH_3)]^{2+}$ ($\mathbf{2}^{2+}$) showing 20% probability of thermal ellipsoids.

peaks, which were removed by running the program SQUEEZE.[50] The CCDC reference number is 761796 for **2**.

Results and Discussion

Synthesis. The ruthenium(II) mixed chelates (**1**−**7**) have been straightforwardly prepared in fairly good yields (40−65%) by reacting $[(H_2pbbzim)RuCl_3]$ with the 4′-substituted terpyridine derivatives in ethylene glycol in the temperature range 190−200 °C under nitrogen protection and then precipitating the complexes either as hexafluorophosphate or perchlorate salts. Temperature was found to be a key factor for the synthesis of the metal complexes. The compound was then subjected to silica gel column chromatography using acetonitrile and 10% aqueous KNO_3 (10:1) as the eluent, followed by a subsequent anion exchange reaction either with NH_4PF_6 or with $NaClO_4$. The compounds were finally recrystallized from an acetonitrile−methanol (1:1) mixture under mildly acidic conditions to keep the benzimidazole NH protons intact. All the compounds have been characterized by their elemental (C, H, and N) analyses, ESI−MS, UV−vis, and ^{1}H NMR spectroscopic measurements, and the results are given in the Experimental Section.

Description of the Crystal Structure of $[(H_2pbbzim)Ru(tpy\text{-}PhCH_3)](ClO_4)_2$ (2). ORTEP representation of $\mathbf{2}^{2+}$ along with the atom labels are shown in Figure 1, and selected bond distances and angles are given in Table 2. The structure displays the expected geometry, with both ligands coordinated in tridentate, meridional fashion to the ruthenium(II) center. The peripheral rings move toward the metal center, as evidenced by a small decrease of the N6−C24−C25 and N8−C30−C29 (for tpy−$PhCH_3$) and N2−C7−C8 and N5−C13−C12 (for H_2pbbzim) angles compared to the ideal angle of 120°. It is to be noted that the interligand angle of the central nitrogen atoms N3−Ru−N7 is 174.49°, whereas the other two angles, N2−Ru−N5 and N6−Ru−N8, are 154.84 and 158.29°, respectively, for this heteroleptic complex. The corresponding angles for the parent $[Ru(tpy)_2]^{2+}$ complex are 178.8°, 158.4°, and 159.1°.[51] The ruthenium−nitrogen bond lengths in tpy-$PhCH_3$ are within 1.936−2.069 Å, whereas in H_2pbbzim they are relatively longer, 2.015−2.088 Å. It is interesting to note that, although the peripheral nitrogen-to-ruthenium bond is similar in the other four instances, the central nitrogen-to-ruthenium bond 1.935 Å (tpy-$PhCH_3$) and 2.015 Å (H_2pbbzim) become shortened. Overall, only small differences in the coordination geometry have been detected when a tpy-X ligand is replaced by H_2pbbzim.

Table 2. Selected Bond Distances (Å) and Angles (deg) for $[(H_2pbbzim)Ru(tpy\text{-}PhCH_3)]^{2+}$ $[\mathbf{2}]^{2+}$

	2
Ru−N(2)	2.086(5)
Ru−N(3)	2.015(6)
Ru−N(5)	2.088(8)
Ru−N(6)	2.069(5)
Ru−N(7)	1.935(5)
Ru−N(8)	2.058(5)
N(2)−Ru−N(3)	77.9(2)
N(2)−Ru−N(5)	154.8(3)
N(2)−Ru−N(6)	92.5(2)
N(2)−Ru−N(7)	101.2(2)
N(2)−Ru−N(8)	92.9(2)
N(3)−Ru−N(5)	77.2(3)
N(3)−Ru−N(6)	106.4(2)
N(3)−Ru−N(7)	174.49(18)
N(3)−Ru−N(8)	95.3(2)
N(5)−Ru−N(6)	91.1(2)
N(5)−Ru−N(7)	103.9(3)
N(5)−Ru−N(8)	92.9(2)
N(6)−Ru−N(7)	79.00(19)
N(6)−Ru−N(8)	158.3(2)
N(7)−Ru−N(8)	79.29(18)

(50) Spek, A. L. *J. Appl. Crystallogr.* **2003**, *36*, 7−13.

(51) (a) Allen, F. H.; Davies, J. E.; Galloy, J. J.; Johnson, O.; Kennard, O.; Macrae, C. F.; Mitchell, E. M.; Mitchell, G. F.; Smith, J. M.; Watson, D. G. *J. Chem. Inf. Comput. Sci.* **1991**, *31*, 187–204. (b) Chartrand, D.; Theobald, I.; Hanan, G. S. *Acta Crystallogr., Sect. E: Struct. Rep. Online* **2007**, *63*, 1561. (c) Schulze, B.; Friebe, C.; Hager, M. D.; Winter, A.; Hoogenboom, R.; Görls, H.; Schubert, U. S. *Dalton. Trans.* **2009**, 787–794.

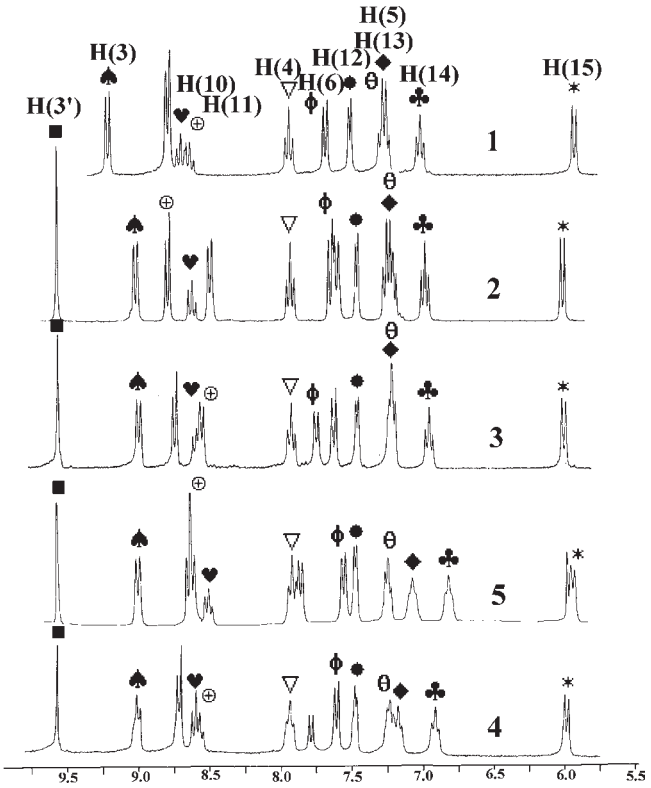

Figure 2. ^{1}H NMR spectra of **1**−**5** in $(CD_3)_2SO$. Atom numbering is shown in Scheme 1.

Scheme 1

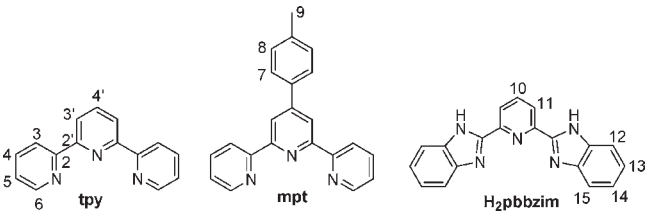

Proton NMR Spectra. ^{1}H NMR spectra of complexes **1**−**7** have been recorded in $(CD_3)_2SO$, and their chemical shift values are given in the Experimental Section. The assignments made for the observed chemical shifts, according to the numbering scheme (shown in Scheme 1), are listed in Table S1 (Supporting Information). The spectral assignments of the complexes have been made with the help of their $\{^1H-^1H\}$ COSY spectra (Figure S2, Supporting Information), relative areas of the peaks, and taking into consideration the usual ranges of J values for H_2pbbzim and tpy-X. Figure 2 shows the ^{1}H NMR spectra of the complexes **1**−**5**.

It is interesting to note that the chemical shift of the CH_2−X proton (H9) of tpy-X in **2**−**6** increases as the substituent, X, is changed in the order CH_3, CH_2Br, CH_2-CN, and $CHBr_2$. Indeed, a linear correlation is obtained (Figure S3, Supporting Information) by plotting $\delta(CH_2-X)$ vs Hammett σ_p parameters (σ_p of $PhCH_3$, −0.17; $PhCH_2Br$:, 0.14; $PhCH_2CN$, 0.18; $PhCHBr_2$, 0.32; and PhCHO, 0.42).[52]

Absorption Spectra. The UV−vis spectral data of the complexes (**1**−**7**) in acetonitrile and the relevant complexes from the literature are given in Table 3. The absorption spectra of all the complexes are similar, showing two very intense bands (ε = 28 000−70 000 M^{-1} cm^{-1}) in the UV region and one moderately intense band (ε = 13 000−23 500 M^{-1} cm^{-1}) in the visible region. The lowest energy band observed between 478 nm (for **1**) and 490 nm (for **5**) can be attributed to metal (dπ)−π*(tpy−X) MLCT transition. The next higher energy band located around 348 nm probably originates from a $\pi-\pi^*$ transition localized at H_2pbbzim. The absorption peaks between 270 and 315 nm are due to $\pi-\pi^*$ ligand centered transitions. It is interesting to note that the peak position of the MLCT band in the complexes undergoes a red-shift, albeit to a small extent with the increase in electron-withdrawing ability of the substituent X.

Luminescence Spectra. The emission spectral behavior of complexes **1**−**7** has been studied at room temperature and 77 K using CH_3CN solutions and methanol−ethanol (1:4) glass, respectively. Table 3 also summarizes the emission maxima, quantum yield (Φ), and lifetime (τ) of the complexes. All the complexes on excitation at their MLCT absorption maximum exhibit one broad luminescent band, which lies between 662 (**1**) and 700 nm (**7**) at 300 K and between 638 (**1**) and 675 nm (**7**) at 77 K (Figure 3) depending upon the substituents in the terpyridine ligand. The bands have the characteristics of emission from the ^{3}MLCT excited state, which corresponds to a spin-forbidden Ru(dπ) → tpy-X(π*) transition.[13−16] In solution, at room temperature, all of the complexes are weak emitters, with their quantum yields ranging from 9.5×10^{-4} to 7.2×10^{-3}. Excitation spectra showed the measured emission signals to be due to the complexes under evaluation. The most striking feature of this class of compounds is that they are luminescent at room temperature in fluid solutions, though the parent $[Ru(tpy/tpy-PhCH_3)_2]^{2+}$ [28] or $[Ru(H_2pbbzim)_2]^{2+}$ [40a,b] are non-luminescent. The room-temperature lifetimes of the complexes which lie between 9 (**1**) and 58 ns (**7**) are significantly greater than that of parent $Ru(tpy)_2$ (0.25 ns) and increase with electron withdrawing substitution in the phenyl group of the tpy-X moiety. In fact a linear correlation can be obtained by plotting the lifetime (τ) vs the Hammett σ_p parameters (Figure 4a). A linear correlation is also obtained between the energies of the emission band maxima (both at room temperature and at 77 K) vs Hammett σ_p plot (Figure 4b). It should be noted that the enhanced luminescence properties of the complexes have been achieved without lowering the excited-state energy significantly. On going from fluid solution to frozen glass, the emission maxima gets blue-shifted with a significant increase of emission intensity and quantum yield (Φ = 0.15−0.20). The blue shift of the emission band on passing from fluid solution to a rigid matrix is typical of MLCT emitters and is mainly due to the inability of frozen solvent to reorganize around the excited molecules. The enhancement of intensity on lowering of the temperature results from slowing down the radiationless transitions, including the thermally activated population of short-lived, upper-lying excited states.[13−16] The free ligand, H_2pbbzim, on excitation at 300 nm fluoresces strongly (Φ = 0.5) at 382 nm in acetonitrile.

To understand the effect of the 2,6-bis(benzimidazole-2-yl)pyridine (H_2pbbzim) ligand along with the different electron-withdrawing substituents in the 4′ position of the *p*-tolylterpyridine moiety, it is useful to recall that the excited-state lifetimes of Ru(II) polypyridine complexes

(52) Hansch, C.; Leo, A.; Taft, R. W. *Chem. Rev.* **1991**, *91*, 165–195.

Table 3. Spectroscopic and Photophysical Data in acetonitrile Solutions for **1**−**7**

		luminescence, 298[a]					luminescence, 77 K[b]	
compd	absorption λ_{max} nm (ε, M^{-1} cm^{-1})	$\lambda_{max\ nm}$	τ, ns	Φ ($\times 10^{-3}$)	k_r, s^{-1} ($\times 10^5$)	k_{nr}, s^{-1} ($\times 10^6$)	$\lambda_{max\ nm}$	Φ
1[c]	478(15700) 348(47300) 313(68700) 271(41800)	662	9.1	0.94	1.0	109.5	638	0.15
2	487(18000) 348(34500) 313(56300) 285(48300)	675	14.8	1.91	1.3	67.4	650	0.16
3	488(13100) 348(28400) 313(40500) 285(28500	688	34.0	2.10	0.6	29.4	661	0.17
4	486(19900) 348(39300) 314(55400) 285(55500)	690	36.9	2.82	0.8	27.0	664	0.17
5	490(23500) 348(49500) 314(63000) 286(63700)	696	50.0	5.04	1.0	19.9	671	0.18
6	488(22600) 348(44700) 313(62600) 286(62900)	691	42.5	3.70	0.9	23.4	669	0.19
7	489(18100) 347(38000) 315(50000) 287(52000)	700	57.5	7.21	1.3	17.3	675	0.20
8[d]	474(10400)	629	0.25	≤0.05	0.04	90.9	598	
9[e]	490(28000)	640	< 5.0				628, 681 (shoulder)	
10[f]	475(17400)							

[a] In CH_3CN. [b] In MeOH−EtOH (1:4) glass. [c] ref 40c, 40d. [d] $[Ru(tpy)_2]^{2+}$, ref 29. [e] $[Ru(tpy\text{-}Ph\text{-}CH_3)_2]^{2+}$, ref 15. [f] $[Ru(H_2pbbzim)_2]^{2+}$, ref 40a.

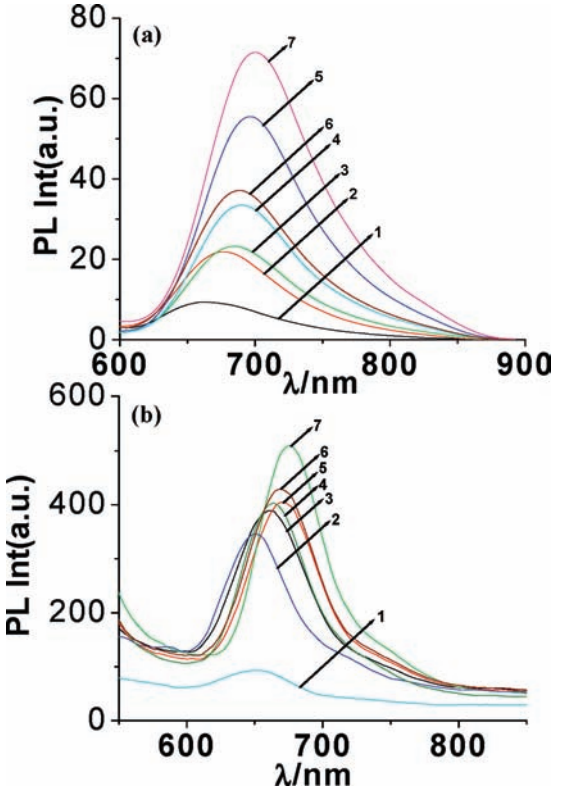

Figure 3. Photoluminescence spectra of the sensors **1**−**7** at room temperature in acetonitrile (a) and at 77 K in ethanol−methanol (4:1) glass (b).

are governed by the nonradiative decay rate constant k_{nr}, given by eq 2[13−15,30]

$$k_{nr} = k_{nr}^{0} + k_{nr}' \quad (2)$$

The overall radiationless decay is the sum of two terms. The first one, k_{nr}^{0}, is directly related to the energy transfer from the MLCT state to the ground state, whereas the second term, k_{nr}', is related to the thermally activated process that takes into account a surface-crossing from the lowest-lying MLCT state to a closely lying metal-centered (MC) level and therefore depends upon the energy gap ΔE between MLCT and MC states.[13−15,30] For Ru(II) complexes with tridentate ligands, the second term normally dominates the equation. The small ΔE between MLCT and MC states in Ru(II) tridentate polypyridine complexes, a consequence of the reduced ligand field strength experienced by the metal center compared to Ru(II) bidentate polypyridine ligands, is due to an ill-fitted octahedral arrangement, which in turn is responsible for the poor room-temperature luminescence properties of $Ru(tpy)_2$-type complexes.[13−15,30]

On plotting ln k_{nr} versus E_{em}^{max}, a linear relationship with a positive slope is obtained (Figure 5).[30,53] This finding probably confirms that the dominant term for k_{nr} in this series of complexes is due to the second term of eq 2.[30,53] Further, the energy of the MC level being considered

(53) (a) Caspar, J. V.; Kober, E. M.; Sullivan, B. P.; Meyer, T. J. *J. Am. Chem. Soc.* **1982**, *104*, 630–632. (b) Chen, P.; Meyer, T. J. *Chem. Rev.* **1998**, *98*, 1439–1478.

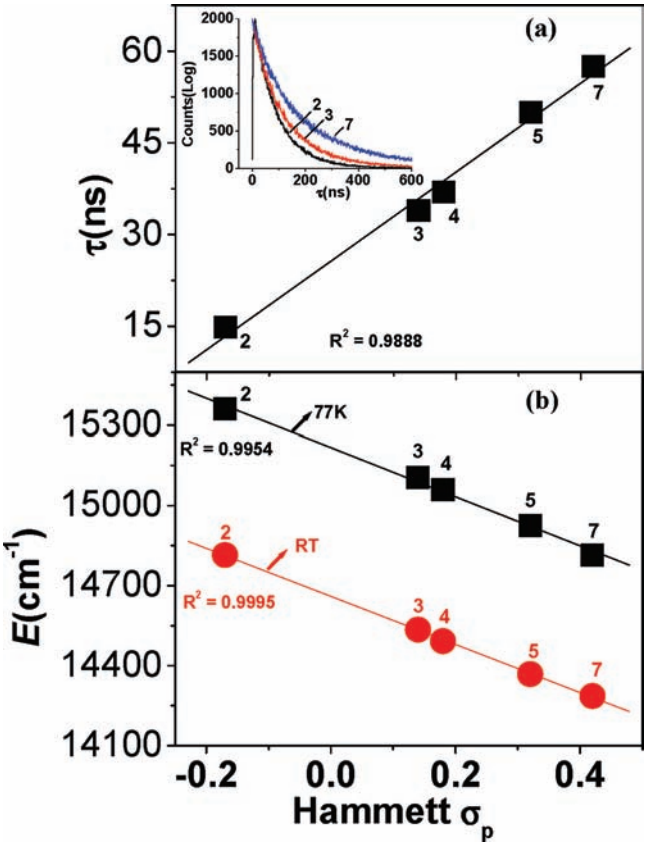

Figure 4. Plot of lifetime (a) and energy of emission maxima (b) vs Hammett σ_p parameters with linear least-squares fit to the data.

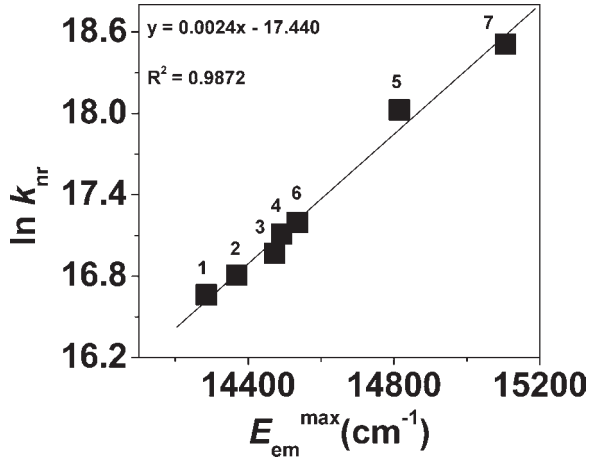

Figure 5. Plot of ln k_{nr} vs E_{em}^{max} for the complexes **1**−**7** at room temperature.

to be constant within the series, the MLCT emitting level is decreased in energy by modulating the electron-withdrawing influence of the substituent in the 4′ position of the *p*-tolylterpyridine moiety. Therefore, this linear relationship probably denotes the reduced efficiency of the MLCT-to-MC surface-crossing pathway as the MLCT excited-state energy is decreased. However, the larger energy gap between MLCT and MC states may not be the only reason to fully justify the relatively long luminescence lifetimes of the complexes. The complete kinetic schemes of the excited state deactivation of these complexes could be much more complicated, and for a better understanding, detailed temperature-dependent photophysical measurements will be required. Unfortunately, due to the lack of such a needed facility, we are unable to address this issue presently.

Table 4. Electrochemical Data[a] for the Complexes **1**−**7** in Acetonitrile

compd	oxidation[b] $E_{1/2}$(ox), V	reduction[c] $E_{1/2}$(red), V
1	0.94	−1.49, −1.90, −2.07
2	1.01	−1.48, −1.86, −2.02
3	1.07	−1.48, −1.82, −2.01
4	1.08	−1.48, −1.82, −2.01
5	1.12	−1.47, −1.79, −2.05
6	1.09	−1.47, −1.82, −2.03
7	1.15	−1.47, −1.78, −1.99

[a] All the potentials are referenced against the Ag/AgCl electrode with $E_{1/2}$=0.36 V for the Fc/Fc^+ couple. [b] Reversible electron transfer process with a Pt working electrode. [c] $E_{1/2}$ values obtained from square wave voltammetric (SWV) using glassy carbon electrode.

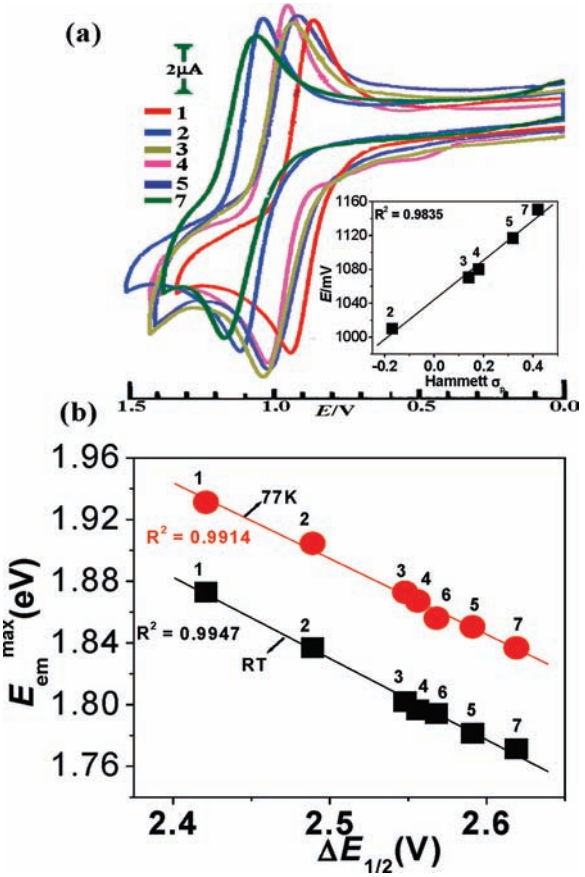

Figure 6. (a) Cyclic voltammograms of **1**−**7** in acetonitrile showing oxidation up to 1.5 V. Inset shows the plot of $E_{1/2}$ vs Hammett σ_p parameters. (b) Plot of $\Delta E_{1/2}$ vs energy of emission maxima.

Redox Properties. The redox activities of complexes **1**−**7** have been studied in acetonitrile solution, and the relevant electrochemical data are given in Table 4. In all the cases, the metal-centered oxidations take place reversibly. A comparison of the electrochemical data reveals that the $E_{1/2}$ values of the complexes increase with an increase in the electron-withdrawing ability of the substituent X, and a linear correlation is obtained by plotting the $E_{1/2}$ values of the Ru^{II}/Ru^{III} couple against the Hammett σ_p parameters (Figure 6a). The complexes are also found to undergo three successive one-electron reversible reductions in the potential

Figure 7. Color changes that occur when the acetonitrile solutions of the receptors **4** (a) and **6** (b) are treated with various anions as their tetrabutylammonium (TBA) salts.

window of 0 to −2.2 V. As the oxidation process is involved in the dπ (t_{2g}) metal orbital and the first reduction process is involved in the terpyridine π^* orbital, a linear correlation is also obtained by plotting the lowest energy MLCT emission maxima and the difference between the oxidation and the first reduction ($\Delta E_{1/2}$) potentials (Figure 6b). The general trend indeed shows an increase in emission energies with increasing $\Delta E_{1/2}$.

Anion Sensing Studies of the Metalloreceptors. Colorimetric Signaling. The anion sensing ability of receptors **1**−**7** has been studied on a qualitative basis by visual examination of the anion-induced color changes in acetonitrile solutions (5×10^{-5} M) before and after the addition of an anion. TBA salts of F^-, Cl^-, Br^-, I^-, NO_3^-, ClO_4^-, AcO^-, and $H_2PO_4^-$ ions have been used as substrates for the receptors. The photograph in Figure 7 shows the dramatic color changes of **4** and **6** in the presence of F^-, AcO^-, and to a lesser extent $H_2PO_4^-$, while in contrast the anions Cl^-, Br^-, I^-, NO_3^-, and ClO_4^- induce almost no change in color. Evidently, there is strong interaction (see later) between the receptors with the substrate anions F^-, AcO^-, and $H_2PO_4^-$ and very weak or no interaction with the other anions.

Absorption Signaling. Sensing of the anions by the metalloreceptors has been monitored by observing the spectral changes that occur in acetonitrile solutions. As shown in Figure 8a, the MLCT peak at 488 nm remains practically unchanged upon the addition of 5 equiv of Cl^-, Br^-, I^-, NO_3^-, and ClO_4^- ions to 2.5×10^{-5} M solutions of **3**. On the other hand, following the addition of 5 equiv of F^- and AcO^-, the said MLCT band gets red-shifted to 525 nm, indicating that strong interactions occur between the receptors and anions. On the addition of $H_2PO_4^-$ though, the MLCT bands of **3** initially shifted to 505 nm, but the addition of excess $H_2PO_4^-$ leads to the precipitation of the resulting complex. These observations are in consonance with the visual changes already noted in Figure 7. The red shift of the MLCT bands can be attributed to the second-sphere donor−acceptor interactions between metal coordinated H_2pbbzim and the anions.[54] Such interactions (hydrogen bonding or proton transfer, vide infra) increase the electron density at the metal center, leading to lowering of the MLCT band energies.

In order to get quantitative insight into sensor−anion interaction, spectrophotometric titrations have been carried out with F^-, AcO^-, and $H_2PO_4^-$ ions. Typical absorption spectral changes for $[(H_2pbbzim)Ru(tpy\text{-}PhCH_2Br)](ClO_4)_2$ (**3**) over the 0−8 equiv range of anions are shown in Figure 9. On close inspection of the changes in the spectral profiles with the incremental addition of anions, the occurrence of

(54) Balzani, V.; Sabbatini, N.; Scandola, F. *Chem. Rev.* **1986**, *86*, 319–337.

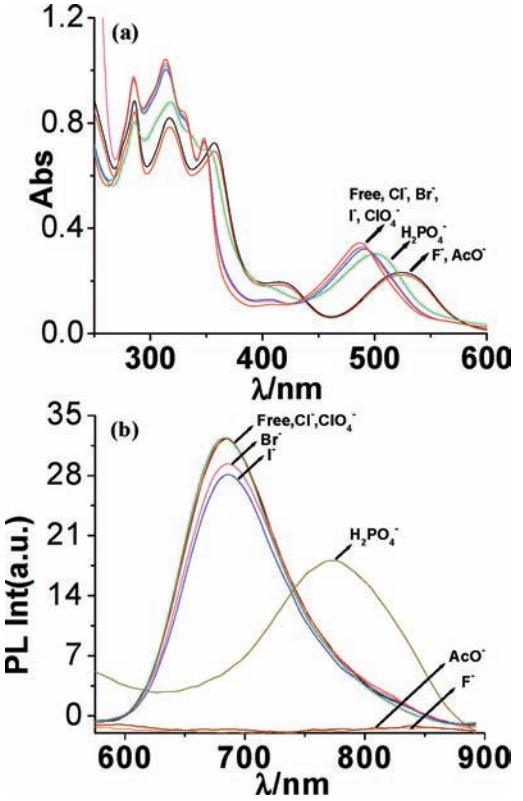

Figure 8. Changes in UV−vis (a) and luminescence (b) spectra of receptor **3** in acetonitrile upon the addition of different anions as TBA salts.

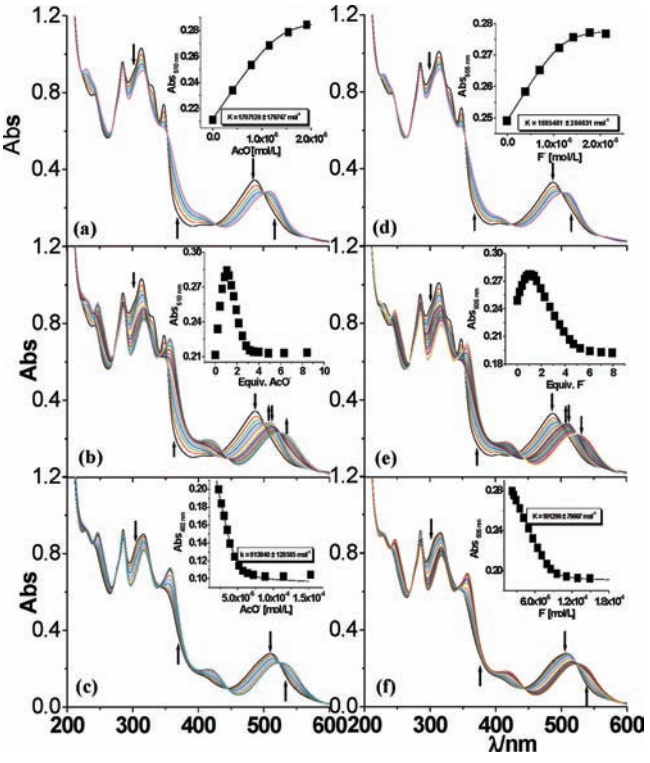

Figure 9. Changes in UV−vis spectra of sensor **3** in acetonitrile upon the addition of AcO^- (a−c) and F^- (d−f). The inset shows the fit of the experimental absorbance data to a 1:1 binding profile.

Table 5. Equilibrium/Binding Constants[a,b] (K, M^{-1}) for **1**−**7** and H_2pbbzim towards Various Anions in acetonitrile at 298 K

from absorption spectra

anions	**1**		**2**		**3**		**4**	
	K_1	K_2	K_1	K_2	K_1	K_2	K_1	K_2
F^-	1.58×10^6	9.14×10^5	1.80×10^6	8.02×10^5	1.75×10^6	9.01×10^5	1.75×10^6	8.13×10^5
AcO^-	1.01×10^6	8.10×10^5	1.99×10^6	9.32×10^5	1.71×10^6	8.14×10^5	1.81×10^6	8.13×10^5
$H_2PO_4^-$	1.13×10^6	NA[d]	1.21×10^6	NA	1.49×10^6	NA	1.35×10^6	NA
	5		**6**		**7**		H_2pbbzim[c]	
	K_1	K_2	K_1	K_2	K_1	K_2	K_1	K_2
F^-	1.12×10^6	8.12×10^5	2.09×10^6	8.87×10^5	2.24×10^6	1.08×10^6	7.00×10^4	NA
AcO^-	2.08×10^6	8.78×10^5	1.44×10^6	7.98×10^5	2.35×10^6	8.85×10^5	4.50×10^4	NA
$H_2PO_4^-$	7.08×10^5	NA	1.48×10^6	NA	1.74×10^6	NA	NA	NA

from emission spectra

	1		**2**		**3**		**4**	
	K_1	K_2	K_1	K_2	K_1	K_2	K_1	K_2
F^-	1.28×10^6	9.24×10^5	1.77×10^6	7.82×10^5	2.26×10^6	7.74×10^5	1.68×10^6	7.92×10^5
AcO^-	1.12×10^6	8.50×10^5	1.95×10^6	9.39×10^5	1.70×10^6	7.38×10^5	1.89×10^6	8.53×10^5
$H_2PO_4^-$	9.23×10^5	NA	1.20×10^6	NA	1.25×10^6	NA	1.25×10^6	NA
	5		**6**		**7**		**H_2pbbzim[c]**	
	K_1	K_2	K_1	K_2	K_1	K_2	K_1	K_2
F^-	1.29×10^6	7.82×10^5	2.36×10^6	8.48×10^5	1.94×10^6	1.11×10^6	7.12×10^4	NA
AcO^-	2.34×10^6	8.12×10^5	1.65×10^6	8.11×10^5	2.48×10^6	8.54×10^5	4.23×10^4	NA
$H_2PO_4^-$	7.16×10^5	NA	1.46×10^6	NA	1.60×10^6	NA	NA	NA

[a] *t*-Butyl salts of the respective anions were used for the studies. [b] Estimated errors were < 15%. [c] Estimate, clean binding profiles were not observed. [d] Not applicable.

two successive reaction equilibria becomes evident. In the first case, spectral saturation occurs with the addition of 1 equiv of either F^- or AcO^- (shown in inset of Figure 9), suggesting a 1:1 receptor−anion interaction, while for the attainment of the second equilibrium process, an excess of anions is required. The spectral patterns of **3** toward the $H_2PO_4^-$ ion are almost the same as those of either F^- or AcO^- up to 1 equiv with two sharp isosbestic points at 496 and 433 (Figure S4, Supporting Information). On further addition of $H_2PO_4^-$ beyond 1 equiv, no noticeable changes in the spectral profile occur, and finally the precipitation of the resulting complex occurs. The absorption spectral profile of all the complexes is basically similar except the position and intensity of the band maxima and follows the same trends with the increasing concentration of the anions (Figure S5−S6, Supporting Information). By using eq 1, the equilibrium constant K for receptor−anion interaction has been evaluated, and the values are given in Table 5.[55] It may be noted that the values of K for the receptors **1**−**7** with F^-, AcO^-, and $H_2PO_4^-$ are grossly over 6 orders of magnitudes.

It was reported previously that suitably substituted H-bond donor receptor functionality undergoes deprotonation in the presence of excess anions, leading to classical Brønsted acid−base chemistry.[56,57] To examine such a possibility, spectrophotometric titrations of the receptors were also carried out with a solution of TBAOH (Figure S7, Supporting Information). The spectral patterns for the complexes have close resemblance to the spectra of these receptors in the presence of F^- and AcO^- ions.

It would be of interest to compare the binding ability of the free H_2pbbzim ligand with its Ru(II) complexes **1**−**7**. In order to do so, spectrophotometric titration experiments were carried out in an acetonitrile solution of H_2pbbzim with various anions (Figure 10). It has been observed that the interactions of the ligand occur only with F^- and AcO^- but not with other anions. Titration of H_2pbbzim was also carried out with the OH^- ion (Figure 10). The titration profile indicates that, with F^- and AcO^-, only one step occurs, while with OH^-, two successive N−H deprotonation steps occur. It may be noted that the binding/equilibrium constants of the metal complexes with the anions are substantially enhanced

(55) Attempts to determine the binding constants of the complexes for anions with 1:2 stoichiometry did not result in any satisfactory fit. The binding constants were obtained by fitting the data to two successive 1:1 equilibrium processes using eq 1.

(56) (a) Kang, S. O.; Powell, D.; Day, V. W.; Bowman-James, K. *Angew. Chem., Int. Ed.* **2006**, *45*, 7882–7894. (b) Gunnlaugasson, T.; Kruger, P. E.; Jensen, P.; Tierney, J; Ali, H. D. P.; Hussey, G. M. *J. Org. Chem.* **2005**, *70*, 10875–10878. (c) Gunnlaugasson, T.; Kruger, P. E.; Jensen, P.; Pfeffer, F. M.; Hussey, G. M. *Tetrahedron Lett.* **2003**, *44*, 8909–8913. (d) Gunnlaugasson, T.; Kruger, P. E.; Lee, T. C.; Parkesh, R; Pfeffer, F. M.; Hussey, G. M. *Tetrahedron Lett.* **2003**, *44*, 6575–6578. (e) dos Santos, C. M. G.; Gunnlaugsson, T. *Dalton Trans.* **2009**, 4712–4721. (f) Peng, X.; Wu, Y.; Fan, J.; Tian, M.; Han, K. *J. Org. Chem.* **2005**, *70*, 10524–10531.

(57) (a) Gomez, D. E.; Fabbrizzi, L.; Licchelli, M. *J. Org. Chem.* **2005**, *70*, 5717–5720. (b) Boiocchi, M.; Boca, L. D.; Gomez, D. E.; Fabbrizzi, L; Licchelli, M.; Monzani, E. *Chem.—Eur. J.* **2005**, *11*, 3097–3104. (c) Amendola, V.; Boiocchi, M; Fabbrizzi, L; Palchetti, A. *Chem.—Eur. J.* **2005**, *11*, 5648–5660. (d) Amendola, V.; Boiocchi, D.; Colasson, B.; Fabbrizzi, L. *Inorg. Chem.* **2006**, *45*, 6138–6147.

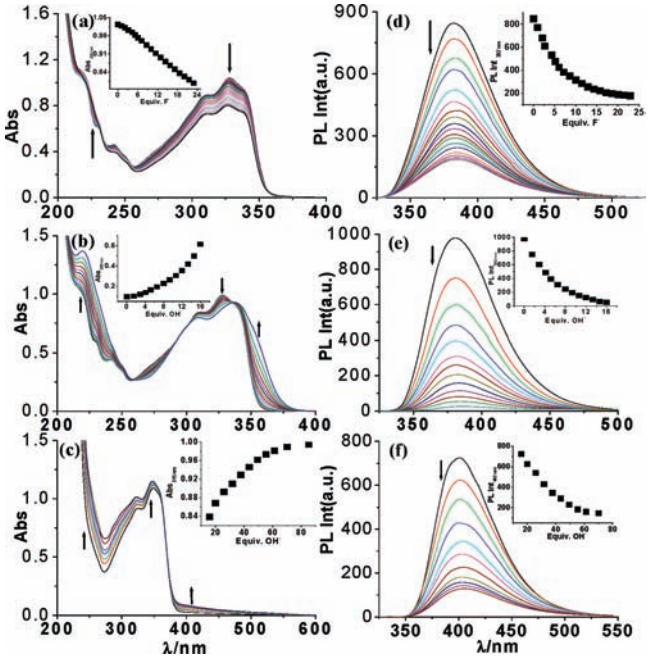

Figure 10. Changes in UV−vis (a−c) and photoluminescence (d−f) spectra of H_2pbbzim in acetonitrile upon the addition of F^- and OH^- ions. The inset shows the absorbance change as a function of the equivalent of anions added.

(2 orders of magnitude) relative to the ligand, H_2pbbzim, itself. We believe this to be caused by the Ru(II) center, which makes the bis-benzimidazole ligand electron-deficient, thereby rendering the imidazole NH's more available for hydrogen bonding to the anions.

Fluorescence Signaling. Figure 8b shows that the emission intensity of the band at 690 nm undergoes nominal change with the addition of Cl^-, Br^-, I^-, NO_3^-, and ClO_4^- ions. On the other hand, with the 5-fold addition of the anions F^-, AcO^-, and $H_2PO_4^-$, the emission intensity gets significantly quenched with a consequent red shift of the emission maximum from 690 to 740 nm, except with $H_2PO_4^-$. Thus, the absorbance and luminescence behavior of the anions show close parlance. Though, in the presence of a large excess of F^- and AcO^-, the room temperature emission of all the complexes gets completely quenched, there is still some residual emission when the measurements are carried out at 77 K (Figure S8, Supporting Information). Photoluminescence titrations of the receptors with various anions have been carried out in the same way as already described for spectrophotometric measurements. In Figure 11, the effect of incremental addition of F^- and AcO^- to **1** is shown, and the inset shows that quenching of luminescence intensity vs the equivalents of anions added. Table 5 also summarizes all of the emission data-derived equilibrium constants measured for the receptors toward different anions. Spectrofluorometric titrations of the complexes were also carried out with TBAOH. The spectral patterns have a close resemblance to the spectra of the receptors in the presence of anions. The emission spectral profile of H_2pbbzim as a function of F^- and AcO^- and OH^- has already been shown in Figure 10. The initial emission peak at 382 nm decreased in intensity gradually and completely quenched after the addition of around 16 equiv of OH^-. Further addition of OH^- leads to an abrupt evolution of a

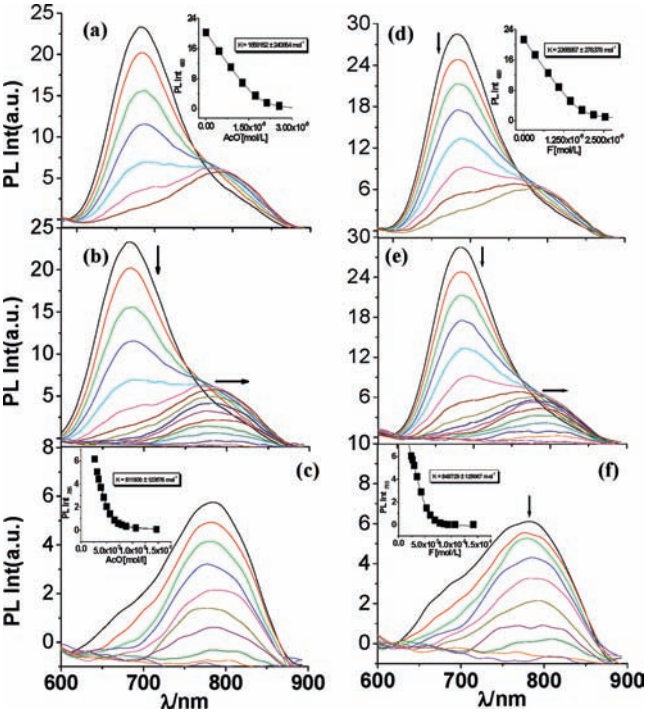

Figure 11. (a) Changes in photoluminescence intensity of the sensor **6** in acetonitrile upon the addition of AcO^- (a−c) and F^- (d−f) ions. Inset shows the fit of the experimental emission data to a 1:1 binding profile.

new emission peak of high intensity at 402 nm and then again gradual quenching of the band.

^{1}H NMR Signaling. ^{1}H NMR spectra of the complexes (**1**−**7**) in the presence of 5 equiv of anions were also recorded (Figure S9, Supporting Information), and the chemical shift values are collected in Table S2 (Supporting Information). It may be noted that the protons associated with the 2,6-bis(benzimidazole-2-yl)pyridine (H_2pbbzim) ligand in the complexes are all up-field shifted by 0.10−0.54 ppm relative to their precursors in the absence of anions. The pronounced shielding effect probably is a consequence of the increase in electron density of the benzimidazole moiety due to the deprotonation of the imidazole N−H protons. As expected, the chemical shifts of the aromatic protons due to tpy-X ligands differ only to a small extent in the complexes.

Figure 12 shows that, with the incremental addition of TBAAcO, the singlet at δ 15.02 ppm due to two N−H groups of H_2pbbzim get broadened, get down-field shifted, and finally vanish when almost 1 equiv of AcO^- was added to a DMSO-d_6 solution of **7**, while the chemical shifts of C−H protons of H_2pbbzim (H_{10}, H_{11}, H_{12}, H_{13}, H_{14} and H_{15}) get progressively up-field shifted. Figure S10 (Supporting Information) shows that the change of chemical shifts for the above benzimidazole protons as a function of the equivalents of AcO^- added, and the chemical shift values of different protons with varying amount of AcO^- are summarized in Table S3 (Supporting Information). A similar behavior was also found with F^- ions. But with $H_2PO_4^-$, the same titration was not successful due to the precipitation of the complex on addition of the anion.

Electrochemical Signaling. Because of the solubility limitation of the receptors in pure acetonitrile, the electrochemical measurements of the receptors with anions were carried out in acetonitrile−dimethylformamide (9:1)

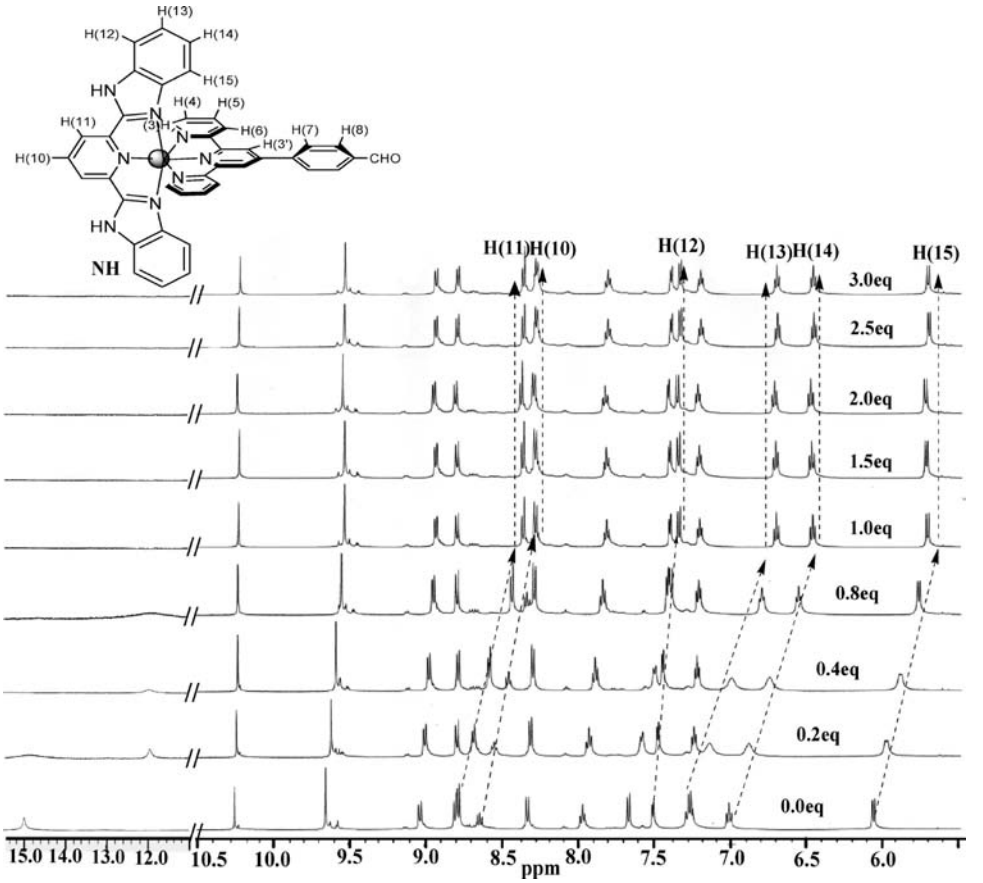

Figure 12. ^{1}H NMR titration of sensor **7** in DMSO-d_6 solution (5.0×10^{-3} M) upon the addition of AcO^- ions (0−3 equiv).

solutions. As shown in Figure 13, with the progressive addition of F^- to **7**, the current height of the redox couple observed at 0.96 V gradually diminishes, and at its expense, a new couple that appears at 0.41 V grows in current heights. As the F^- ion concentration reaches 3 equiv, the couple at 0.96 V is completely replaced by the 0.41 V couple. The electrochemical behavior observed with AcO^- as the guest anion is almost identical to that of F^- for all the receptors (Figure S11, Supporting Information). A closer examination of the current versus equivalent of anions plot shows that, in the intermediate range, a steady decrease or increase of current occurs in two steps with a plateau around 1 stoichiometric equiv of anion, indicating the presence of two successive equilibrium processes. Thus, the progressive addition of anions to the solution of the receptors resulted in a negative shift of the oxidation potential, demonstrating a strong interaction between the receptors and anions. It should be noted that the redox potentials of the complexes in pure acetonitrile, as reported earlier, differ from those obtained in an acetonitrile−dimethylformamide (9:1) medium due to a solvent effect. With $H_2PO_4^-$, the electrochemical behavior became complicated due to adsorption and poisoning of the electrode surface. In contrast to F^- and AcO^-, no noticeable changes occur in electrochemical responses for the receptors in the presence of a large excess of Cl^- and NO_3^-. The results presented here provide a hint that the complexes **1**−**7** could prove useful in the fabrication of electrochemical sensors.

Nature of Receptor−Anion Interaction. The observations made above from ^{1}H NMR, photometric, luminescence, and electrochemical measurements unequivocally suggest that F^-, AcO^-, and to some extent $H_2PO_4^-$ ions interact strongly with the metalloreceptors **1**−**7** in 1:1 stoichiometry, albeit such interaction is either very weak or absent for other halides (Cl^-, Br^-, I^-) and oxyanions (NO_3^- and ClO_4^-). The close resemblance of both absorption and emission spectral patterns of the receptors in the presence of OH^- to those in the presence of F^- and AcO^- ions suggest that metal-coordinated H_2pbbzim in **1**−**7** gets successively deprotonated to Hpbbzim^{-1} and finally to pbbzim^{-2} in the presence of an excess of anions. It would appear at first that the role of the anions F^- and AcO^- is simply to abstract the N−H protons according to eq 3:

$$\begin{aligned}[(\text{tpy-X})\text{Ru}^{\text{II}}(\text{H}_2\text{pbbzim})]^{2+} &\overset{-\text{H}^+,\,K_1}{\rightleftharpoons} \\ [(\text{tpy-X})\text{Ru}^{\text{II}}(\text{Hpbbzim})]^{+} &\overset{-\text{H}^+,\,K_2}{\rightleftharpoons} \\ [(\text{tpy-X})\text{Ru}^{\text{II}}(\text{pbbzim})]\end{aligned} \qquad (3)$$

However, there is growing evidence suggesting that the picture could be far from simple.[1,2,5,48] It appears that hydrogen bonding, supramolecular interaction of a second coordination sphere, and a proton transfer reaction probably come into play. In the present case, we envisage that the imidazole N−H protons of the receptors interact with selective anions X^- (F^-, AcO^-, and to some extent $H_2PO_4^-$) to form an incipient N−H···X^- hydrogen bond, and the presence of an excess of X^- induces further stretching of the N−H bond, which eventually splits through a proton transfer reaction as shown in Scheme 2.

Scheme 2

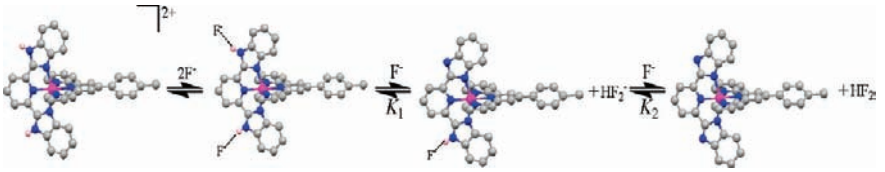

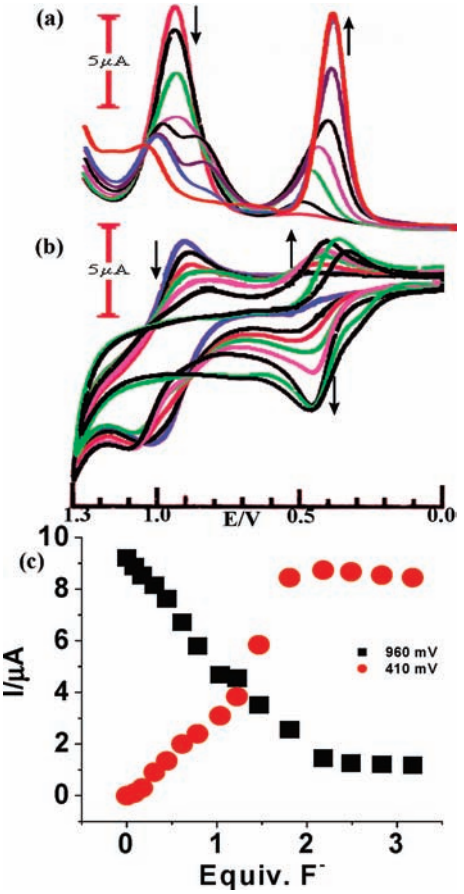

Figure 13. SWVs (a) and CVs (b) of receptor **7** obtained upon incremental addition of TBAF to an acetonitrile−dimethylformamide (9:1) solution (1.0×10^{-3} M). The changes in the current intensities as a function of equivalents of F^- are shown in c.

It has been argued that the higher stability of a polynuclear aggregate, such as HF_2^-, further facilitates the deprotonation of the receptor unit. It is interesting to note that the stepwise deprotonation process is fully reversible, as indicated by the fact that, on the progressive addition of water, the violet color of the acetonitrile solutions of the receptors first turns orange red and then the original yellow-orange. Finally, we note that, although the receptors **1**−**7** exhibit a strong response toward sensing F^-, AcO^-, and to a lesser extent $H_2PO_4^-$, they lack selectivity to differentiate these anions explicitly.

Conclusion

In conclusion, we have developed a new series of heteroleptic bis-tridentate ruthenium(II) complexes by using the tridentate ligand 2,6-bis(benzimidazole-2-yl)pyridine (H_2pbbzim) and different 4′-substituted terpyridine derivatives (tpy-X), which can act as multi-channel sensors of anions such as F^- among halides and AcO^- and, to some extent, $H_2PO_4^-$ among oxoanions in solution. To allow fine-tuning of the electronic properties, several electron withdrawing groups have been introduced in the 4′ position of the terpyridine ligand, resulting in seven complexes in total. The most striking feature of this class of compounds is that they are luminescent at room temperature in fluid solutions, and their room temperature lifetimes lie in the range of 10−58 ns. The sub-nanosecond excited-state lifetime of normal tpy complexes is widely accepted as being due to the small energy gap between the emitting ^{3}MLCT state and the deactivating ^{3}MC level. The important outcome of this study has been to increase the energy level separation of the two states by modulating the ^{3}MLCT energy level of the complexes by varying the electronic influence of the substituent X in the 4′ position of the tpy unit, while keeping the energy of the ^{3}MC state essentially unchanged. Another point of interest is that the emitting properties of the compounds are determined by the protonation state of the benzimidazole rings. This opens the possibility of the application of such compounds as proton driven molecular switches. Correlations between the Hammett σ_p parameter and MLCT emission energies, room temperature lifetime, the potentials of the oxidation and reduction processes, ^{1}H NMR chemical shifts, etc. show that the greater the electron accepting ability of the substituents, X, the greater the stabilization of the LUMO π^* ligand centered orbital of tpy-X than the HOMO $\pi(t_{2g})$ metal orbital. The binding properties are also confirmed by absorption, emission, and ^{1}H NMR spectroscopic and cyclic voltammetric techniques. From binding studies, it has been concluded that, at a relatively lower concentration, 1:1 H-bonded adducts between the metalloreceptors and the anions are formed, while in the presence of excess anions, stepwise deprotonation of the two benzimidazole N−H fragments occurs, an event which is signaled by the development of intense and beautiful colors visible with the naked eye. Cyclic voltammetry (CV) studies carried out in acetonitrile−dimethylformamide (9:1) have provided evidence of anion-dependent electrochemical responses with F^- and AcO^-, rendering complexes **1**−**7** as suitable electrochemical sensors.

Acknowledgment. Financial assistance received from the Department of Science and Technology, New Delhi [Grant No. SR/S1/IC-06/2006] and the Council of Scientific and Industrial Research, New Delhi, India [Grant No. 01(2084)/06/EMR-II] is gratefully acknowledged. Thanks are due to the Department of Inorganic Chemistry of the Indian Association for the Cultivation of Science, Kolkata, India, for single crystal X-ray data. C. B., S.D., and D.S. thank CSIR for their fellowship.

Supporting Information Available: X-ray crystallographic file in CIF format for compound **2**, Tables S1−S3, and Figures S1−S12. This material is available free of charge via the Internet at http://pubs.acs.org.